Aus der Neurologischen Klinik und Poliklinik
der Ludwig-Maximilians-Universität München

Direktorin: Prof. Dr. med. Marianne Dieterich

Rapid Motor Responses to External Perturbations During Reaching Movements: Experimental Results and Modelling

Dissertation
zum Erwerb des Doktorgrades der Humanbiologie
an der Medizinischen Fakultät der
Ludwig-Maximilians-Universität zu München

vorgelegt von
Lei Zhang

aus
Harbin/China

2015

Mit Genehmigung der Medizinischen Fakultät

der Universität München

Berichterstatter:	Prof. Dr. Andreas Straube
Mitberichterstatter:	Priv.-Doz. Dr. Ingo Borggräfe
	Priv.-Doz. Dr. Dieter Kutz
Mitbetreuung durch den promovierten Mitarbeiter:	Dr.-Ing. Thomas Eggert
Dekan:	Prof. Dr. med. Dr.h.c. Maximilian Reiser, FACR, FRCR
Tag der mündlichen Prüfung:	13.07.2015

Abstract

One critical nature of the human motor system is that it is able to maintain stability of voluntary movements that are unexpectedly disturbed. In many cases the disturbance is automatically and rapidly cancelled out, even before it appears in conscious awareness that a particular action is needed to avoid a fall after stumbling over a stone during walking, or to prevent from spilling the wine out of the glass when the holding arm is suddenly bumped by someone at a cocktail party.

These immediate reactions after a disturbance are initially activated by the peripheral motor system, including the muscles themselves and a neural pathway between spinal cord and the muscles. This thesis focuses on the function of these peripheral mechanisms at compensating for unexpected mechanical perturbations of the motor system.

The first study explored the characteristics of initial motor responses to unexpected perturbations during unconstrained arm reaching movements. While most previous experiments have investigated two degrees-of-freedom (DoFs) reaching movements involving only elbow and shoulder joints, a seven-DoF arm has inherent and high complexity and instability. By recording the seven-DoF arm motion and calculating movement variables, this study showed that key movement features of 2D-arm movements, such as bell-shaped hand velocity and biphasic joint torque, were mostly preserved during natural unconstrained movements. The study further indicated that the motor responses that start shortly after the perturbation contribute to system stabilization. These results suggest that the rapid compensatory responses to small perturbations are dominated by peripheral mechanisms.

The second study has taken the functional details of these mechanisms into account and examined whether they can cope efficiently with small perturbations. A single-joint model with one antagonistic muscle pair was implemented, capturing essential features of the physiology of the peripheral system. The experimental situation was simulated and the predicted results of the simulation were compared to the measured perturbation consequences. There was a considerable consensus between the predicted movement and the measured one, with perturbations being induced at different phases of the reaching movement. It is concluded that the peripheral mechanisms can be sufficient at

compensating for small perturbations of arm movements. Furthermore, simulation results with altered mechanical parameters of the model suggest that different components of the peripheral mechanisms cooperate in a synergistic way during the compensation process.

Above all, human motor system is able to generate rapid responses to correct movements that are unexpectedly perturbed. Small perturbations can be sufficiently compensated by peripheral mechanisms alone. This allows understanding more deeply how the central motor system is able to control complex movements and how these goal-directed movements can be stabilized even during unexpected perturbations of the effector. This thesis provides an efficient methodology to quantify perturbation responses during unconstrained reaching movements and it points out the important role of peripheral mechanisms in movement stabilization.

Contents

1. General Introduction

"To move things is all that mankind can do, for such the sole executant is muscle, whether whispering a syllable or felling a forest."

Sir Charles Sherrington

How can we human beings move? From simple movements such as reaching to grasp a cup of coffee, to more complex movements such as piano playing, all kinds of motor actions result from contracting muscles. The muscles are innervated by neural signals through the spinal cord downstream from the central commander – our brain. The brain, together with the spinal cord, composes the central nervous system (CNS). How the CNS organizes different muscles to produce both natural and adaptive movements is a complex problem, and this question is of central interest and being extensively investigated in the field of human motor control. Discovering the motor control mechanisms not only provides insights to the normal functionality of CNS but also can explain the dysfunction of motor system and help treat motor diseases.

There are different approaches to study human motor control and the discussions in the field have been controversial. Over a century ago, the neurophysiological foundation of human motor control was set by Sir Charles Sherrington, who has demonstrated the spinal-level reflex mechanisms (Sherrington 1906). After that, many influential ideas of motor control have emerged and contributed to the development of the field. One important idea is that movement is centrally organized by certain patterns or general rules, encoded as the motor program which is stored in the brain (Bernstein 1967, Schmidt 1975). Inspired by control engineering approach, this idea was further formulized as internal models (Wolpert et al. 1998, Kawato 1999) that combine feedforward control (i.e. predefining control signals) and state estimation by cooperating peripheral sensory signals and a copy of motor

commands (Von Holst and Mittelstaedt 1950). Contemporary development of motor control theories is mainly divided into two directions. One direction roots in the motoneuron physiology based on Sherrington's reflex theory and it highlights the role of the low-level motor system which takes over the burden of the brain for motor control (see Equilibrium Point Hypothesis in section 1.1), while the other direction, inspired by theories of control engineering, focuses on the computational nature of the CNS (see Optimal Feedback Control in section 1.1).

To interact with the external world, motor control has to be successful to achieve the behavioral goal. If actions are disturbed, the motor system can adjust and generate corrective responses to ensure a good performance. This thesis focuses on the stability properties of the motor system during reaching movements and investigates peripheral motor responses, which are most immediate to tackle with external perturbations, both experimentally and by theoretical simulation. The motivation of studying peripheral system is briefly introduced in section 1.2. When encountering a perturbation, at least initially the peripheral motor system may play a significant role in movement stabilization, since the spinal loops have smaller latencies than the supra-spinal loops. The question is how efficient are the most immediate responses for movement stabilization and what are the underlying control mechanisms? Do these control mechanisms for low-dimensional movements also hold for high-dimensional movements? In section 1.2, we will have a literature review of related studies adopting mechanical perturbations to probe motor control. In section 1.3, the objectives of this thesis will be given.

1.1 Theories of motor control

Motor control is a relatively young field in biological science and has developed rapidly over the past several decades. Unfortunately, there is no motor control theory that is currently accepted by all researchers in the field. Like in other fields of science, a scientific theory (such as quantum mechanics in physics) becomes mature only when it can be validated through extensive and critical experimental tests. In this section, two of the most important theories of motor control are introduced. Both of them have been tested extensively by behavioral experiments while controversial discussions are still going on.

Equilibrium Point Hypothesis (EPH)

The principle of EPH is based on the argument that stretch reflex is a tunable mechanism (Sherrington 1906) and its parameters can be modulated by descending signals from the brain.

The stretch reflex loop mainly consists of motoneurons (so-called α-motoneurons in the anterior horn of the spinal grey) innervating the muscle and afferent nerves sending the muscle length and velocity signals back to the motoneurons (via the dorsal horn of the spinal grey). The motoneuron is a threshold element. The electrical threshold of the motoneuron membrane potential corresponds to a certain muscle length, which is called threshold muscle length (Feldman 2011). If this threshold length is beyond the actual muscle length, motoneuron does not fire and the muscle is silent. Muscle is activated when the threshold length is below the actual muscle length. Thus, by changing threshold muscle length[1], the CNS can modulate the muscle activity, which depends on the difference between the actual muscle length and the threshold length.

Such mechanism was supported by experiments on decerebrated cats (Matthews 1959, Feldman and Orlovsky 1972). These studies showed that a fixed descending input (induced by a constant stimulation) to the spinal cord led to a resting muscle length (i.e. the stimulation-induced muscle length without external force, or in EPH vocabulary the

[1] There are two ways to change threshold muscle length. One way is to elicit length-dependent motoneuron facilitation by the descending signal, leading to an increase of motoneuron membrane potential, while the electrical threshold of the motoneuron membrane potential remains constant. Thus with the same lengthening of the muscle, motoneuron fires at a shorter threshold length. The other way is to directly change the electrical threshold of the motoneuron membrane potential. For more details see Fig. 2 in Feldman 2011.

threshold muscle length). At this fixed level, by passive stretch of the muscle they obtained a non-linear relationship between muscle length change and evoked muscle force. When the stimulation level changed, this relationship was preserved while only the resting muscle length changed. This confirms that the descending signals can modulate the resting (or threshold) muscle length.

The idea of central modulation of threshold muscle length was further supported by experiments on intact human subjects. Feldman (1966, 1986) instructed the subjects not to intervene voluntarily with an unloading when holding a posture against a load, assuming that during unloading the subject's descending signals remained the same. With different initial joint angles and load changes, Feldman obtained a set of non-linear joint angle-torque curves, which is similar to the muscle length-force relationship observed in the studies on decerebrated cats.

In short summary, based on experimental observations the principle of EPH can be interpreted as central modulation of stretch reflex parameters (such as threshold muscle length). A mathematical implementation of this mechanism is introduced as "model of threshold position control" in section 3.2 of the thesis.

Optimal Feedback Control (OFC)

OFC formulates motor control as a computational problem by finding mathematical solutions to satisfy a certain optimal criterion. In particular, it makes hypotheses about specifying system functions to relevant neural structures (cerebellum, Basal ganglia, etc.) for such control (Shadmehr and Krakauer 2008, Scott 2012). For a given task, OFC compares the performance of the biological system with the best possible theoretical solution for the hypothetical function.

In OFC algorithms (Todorov 2005), there are three key components to specify. First is the task goal, which is defined by a cost function that depends on certain movement parameters, e.g., the distance of a reach endpoint from a target location, or the time or the energy of the movement. The second component is a control law which is derived from that hypothetical goal to minimize the costs. In the simplest case this control law would act on the true states of the motor plant that has to be controlled. However, the true states (e.g.

position and velocity of the hand) cannot be directly assessed by the CNS but only indirectly observed on the basis of sensory afferents. This observation is formalized in OFC as the so-called state estimation, which integrates delayed sensory feedbacks and a copy of motor commands. This estimation process (the third component) can even predict system changes before the arrival of sensory information. All three components form the whole controller which interacts with the musculoskeletal system. The controller sends the motor commands to and receives the sensory information from the musculoskeletal system.

The mathematical form of OFC algorithms is rather complex (Todorov 2005). Numerous behavioral experiments have shown that the CNS possesses good solutions that are OFC-like, while the challenge remains how such OFC-like control can be implemented by the distributed neural circuits in the brain (Scott 2012).

1.2 The importance of peripheral mechanisms

The peripheral mechanisms mainly consist of intrinsic muscle properties and the spinal reflexes. These mechanisms are at low level of motor control in human. At the high (supra-spinal) level, the brain sends control signals to the low-level system and receives the sensory feedbacks from it.

Many recent studies have investigated the top-level mechanisms of motor control in the presence of perturbations. They demonstrated that the intact CNS, especially the cerebellum, is critical for flexible control mechanisms, which can be adaptive to task or environmental changes (Kawato 1999, Shadmehr and Krakauer 2008). Compared to this intelligent control in the top-level, the peripheral control system in the bottom-level seems to be relatively stereotyped and much less “smart”. However, the peripheral motor system has the direct and immediate access to the muscle, the “sole executant” of the movement. In reaction to a perturbation, the peripheral motor system generates the fastest motor responses, while the supra-spinal loop takes an effect later, due to relatively longer delay. Furthermore, the peripheral mechanisms are of significant importance in movement generation. According to EPH, the peripheral system is driven by the top-level control. The top-level control does not directly specify the motor patterns such as kinematics, dynamics or electromyography (EMG) but rather it only sets parameters of the peripheral system (Ostry and Feldman 2003, Feldman and Latash 2005). As a consequence, movement is

generated by interactions among all components of the peripheral system. Impaired functionality of peripheral mechanisms such as loss of proprioception causes abnormal movement trajectories (Sainburg et al. 1995). A recent development of OFC theory also assigns certain "intelligence", a separate control algorithm, to the peripheral controller which affords a fast feedback loop (Todorov et al. 2005). Thus, from both experimental and theoretical perspectives, peripheral mechanisms give important insights into the fundamentals of motor control.

1.3 Review of literatures on perturbation studies

The use of mechanical perturbations is a standard methodology for experimental studies to probe motor control with the peripheral mechanisms. Experimentally, different types of perturbations have been applied to elicit arm motor responses, such as force pulses (Frolov et al. 2006, Gomi and Kawato 1997), position perturbations (Burdet et al. 2000; Darainy et al. 2007) and virtual constrains (Mah 2001). These perturbation studies are typical for measuring arm stiffness. Using load perturbations, Soechting and Lacquaniti performed a series of perturbation studies in the 1980s, to investigate torque and EMG responses during posture and pointing (Lacquaniti and Soechting 1984, 1986a, b; Soechting 1988, Soechting and Lacquaniti 1988). To examine the stretch reflex characteristics, oscillating or random perturbations were also applied in some studies (Bennett 1994, Van der Helm et al. 2002). Most recently, large long-lasting perturbations were used to study motor actions when the arm was strongly destabilized (Zhou et al. 2014).

Most perturbation studies of arm reaching have focused on limited dimensions of the whole arm. In many studies, movements were constrained to two DoFs of shoulder and elbow joints only, mainly on either horizontal or vertical plane. It is unclear whether they also apply to movements in free space, when all seven DoFs of the arm joints are considered. Especially the elbow and shoulder torsions, which add more complexity to the system, may result in an increase of system instability. Several recent studies of full DoF reaching movements focused mainly on the natural movement generation (Grimme et al. 2012, Schütz and Schack 2013) or movement variability (Mattos et al. 2011, Krüger et al. 2012). To the author's knowledge, perturbation response during full DoFs reaching has not been extensively investigated before (see section 2).

To study how peripheral mechanism is centrally modulated during reaching movement, perturbations were applied in different phases of the movement and stretch reflexes were examined. When applied shortly before and in the very early phases of the movement, only strong perturbations were able to elicit a stretch reflex (Adamovich et al. 1997). Studies using relatively weak perturbations suggested that reflex sensitivity was centrally suppressed at the initial phase of the movement (Brown and Cooke 1981, Shapiro et al. 2004, Niu et al. 2012). When perturbations were applied during middle and late movement phases, the stretch reflexes were always observed (Milner 1993, Bennett 1993, Latash 1994, Smeets et al. 2004, Niu et al. 2012), suggesting a significant level of reflex sensitivity after movement start. Previous studies have demonstrated that during movement, motor system can respond to external perturbations very rapidly by evoking stretch reflexes. The question remains, how efficient are the motor responses generated by peripheral control mechanisms in compensating for perturbations (see section 3).

1.4 Thesis objectives

While previous perturbation studies have mainly considered constrained movements with limited DoFs, the first study in this thesis aims to investigate unconstrained movements which are more complex, involving full seven DoFs of the arm in a three-dimensional space. At the first step, certain kinematical and dynamical features of unperturbed full DoFs movements were compared with those of two-joint movements. Such a comparison is to find, to what extent control strategy depends on the complexity of the movement. For dynamical analysis, joint torque was calculated based on an inverse-dynamic approach, using recorded kinematical and force data. At the second step, the motor responses were quantified as the joint torque difference between unperturbed and perturbed movements. The results suggest that these torque responses compensate well for the randomly applied perturbation.

Initial torque responses to perturbations are most likely generated by peripheral motor system because top-level control loop has relatively longer delay. The second study thus focuses on the underlying control mechanisms of the peripheral system in movement stabilization. Torque and EMG responses to transient small perturbations, which were applied at different phases of the movement, were measured and analyzed. To incorporate

experimental observations into a theoretical framework, simulation studies were performed. In the framework of EPH, previous simulation studies have been mainly focused on the generation of natural movements (St-Onge et al. 1997, Gribble et al. 1998, Pilon and Feldman 2006). In the current study, the model of EPH was implemented to predict motor responses to unexpected mechanical perturbations. Due to the complexity of modelling the musculoskeletal structure, the second study of the thesis only considers single-joint movement. A comparison between experimental data and model prediction was made to validate the efficiency of peripheral motor control in movement stabilization.

The remaining parts of the thesis are organized as follows: the second and the third sections present the two studies cumulatively. The fourth section offers a general discussion of the main findings of the thesis. With respect to the topic of this thesis, a third study in which the author has collaborated is also briefly reported in the fourth section.

2. Torque Response to Perturbation During Unconstrained Arm Movements[1]

Abstract

It is unclear to what extent control strategies of 2D reaching movements of the upper limbs also apply to movements with the full seven degrees of freedom (DoFs) including rotation of the forearm. An increase of DoFs may result in increased movement complexity and instability. This study investigates the trajectories of unconstrained reaching movements and their stability against perturbations of the upper arm. Reaching movements were measured using an ultrasound marker system and the method of inverse dynamics was applied to compute the time courses of joint torques. In full DoF reaching movements the velocity of some joint angles showed multiple peaks while the bell-shaped profile of the tangential hand velocity was preserved. This result supports previous evidence that tangential hand velocity is an essential part of the movement plan. Further, torque responses elicited by external perturbation started shortly after perturbation, almost simultaneously with the perturbation-induced displacement of the arm, and were mainly observed in the same joint angles as the perturbation torques, with similar shapes but opposite signs. These results indicate that these torque responses were compensatory and contributed to system stabilization.

[1] Adapted from Zhang L, Straube A, Eggert T (2014) Experimental brain research 232 (4):1173-1184.

2.1 Introduction

In daily life the motor system is able to perform goal-directed movements (e.g. reaching movements) even during unexpected mechanical perturbations, thus demonstrating the intrinsic stability of the motor system (Won and Hogan 1995; Burdet et al. 2006; Hasan 2005). Experimentally a variety of perturbations has been applied, such as force pulses (Frolov et al. 2006; Gomi and Kawato 1997), servo-displacements (Burdet et al. 2000; Darainy et al. 2007), and virtual walls (Mah 2001) to elicit and to quantify the torque as the essential motor response to the perturbation. In these studies, movements were constrained to two degrees of freedom (DoFs) of shoulder and elbow joints only. The subject's arm was elevated, moving in a horizontal plane passing through the shoulder. There are also a few perturbation studies of vertical arm movements. Soechting and Lacquaniti performed a series of studies to explore the effect of load perturbations during posture and vertical pointing (Lacquaniti and Soechting 1984; Lacquaniti and Soechting 1986a; Lacquaniti and Soechting 1986b; Soechting 1988; Soechting and Lacquaniti 1988). These studies showed a high correlation between effects on joint torque changes and the electromyographic (EMG) responses. Again, these movements were confined to 2 DoFs. Most studies observed torque (or force) responses with nonlinear, spring-like properties (Hogan 1985). In the short term (< 50 ms after perturbation), the spring-like dynamic of the human motor system may originate from two different mechanisms. The first mechanism is the intrinsic muscle mechanical properties (Krylow and Rymer 1997), such as muscle stiffness, which is known to have only minimal (<1 ms) delay with respect to changes in muscle length (Cecchi et al. 1986). For the second mechanism the stretch reflex loop, which regulates the muscle activity with a time delay in the order of tens of milliseconds, is discussed (Cargo et al. 1976; Lacquaniti and Soechting 1984).

While most previous experiments investigated movement with two DoFs, they may not necessarily also be applicable to movements in three-dimensional free space, when full DoFs of the arm joints are involved, including the rotation of the forearm. The control strategy during reaching movements using the full seven DoFs of the shoulder, elbow, and wrist could be different from that during 2D reaching because: (1) In a 2D work space with two DoFs, the solution of arm configuration for a given hand position is unique, in the case of seven DoFs there are abundant DoFs for the motor system to attain the same hand position; (2) The dynamics of the unconstrained mechanical system (seven DoFs) are much

more complex than those of the constrained system (two DoFs). Recent studies of 3D arm movements (Grimme et al. 2012; Schütz and Schack 2013) suggested that movement generation can be simplified by its decomposition into motor primitives, in terms of kinematics. Some studies also investigated the dynamics of 3D unconstrained arm movements (Lacquaniti et al. 1986, Biess et al. 2007; Jindrich et al. 2011), considering shoulder and elbow joints with 4 or 5 DoFs. Another field of multi DoF movements is opened by whole body pointing and reaching tasks. Also with these tasks it was shown that movement kinematics (Pozzo 2002; Lee 2008; Berret 2009) and dynamics (Thomas 2005) are subject to motor synergies allowing the motor system to effectively parameterize the movements. However, torque responses of full DoF arm movements to perturbations in 3D space were not extensively studied in the past.

The present study has two objectives. The first goal is to quantify the kinematics and dynamics of unconstrained arm movements with full DoFs during natural reaching in order to determine whether such movements have similar kinematic and kinetic profiles as 2D reaching. For 2D movements bell-shaped hand velocity profiles and biphasic joint torque profiles were shown. The second goal is to quantify joint torques in response to unexpected small transient mechanical perturbation during unconstrained reaching and to determine the role of these fast responses for movement stabilization. We extended an existing setup for kinematic analysis of unconstrained reaching movements (Krueger et al. 2011) to apply nearly impulse-like force perturbations. The perturbation force was small, so that subjects could complete the reaching task without deviating too much from the final target and yet strong enough to cause a measurable effect on the arm trajectory. The current study introduces this experimental setup and the corresponding analysis methods to investigate short-latency perturbation responses to impulse-like force perturbations.

2.2 Methods

Subjects

Ten subjects (seven females and three males, mean age: 32.5±4.1 years, right-handed, without any movement disorders) participated in this study. They had no previous experience with the experimental task and were not aware of the purpose of the study. Written consent was obtained prior to participation in the experiment. The experimental procedure was in accordance with the Declaration of Helsinki and approved by the local Ethics Committee.

Apparatus

The apparatus shown in Fig. 2.1 was used to investigate the arm response against external perturbations. The subject sat on a chair and was instructed to minimize trunk movements during the experiment. A metal ball mounted on the table in front of the subject served as reaching target. The distance between the chair and the table was adjusted so that the subject could grasp the target with the arm almost, but not fully extended. Subjects wore LCD-shutter glasses to prevent visual feedback during the movement.

Arm movement was recorded by a 3D ultrasound-based motion analysis device (Zebris Medical GmbH) at a sampling rate of 33 Hz for each marker. The measurement was based on the travel time of ultrasonic pulses emitted by 6 markers to 3 microphones. The perturbation was applied by attaching a high-stiffness rope to the elbow joint. As shown in Fig. 2.1, one end of the rope was connected to a band around the subject's elbow joint and the other end was connected with a low-stiffness spring, which was fixed on the wall. The middle part of the rope went through a brake, where the rope could be suddenly stopped by a metal pin that could be pulled onto the rope by means of a strong electric magnet. The magnet was controlled by a digital signal which switched the magnet on or off. When the magnet was switched off, the metal pin was immediately released and the rope could pass freely through the brake. The force in the rope was measured by a strain gauge that allowed accurate dynamic force measurement (Rieger, Rheinmünster, Germany). The contact between the hand and the metal ball was detected by the sudden drop of the

electrical resistance between the subject and the ball, measured by the output signal of a voltage divider. Both the force signal and the contact signal were sampled at 1 kHz.

A computer with a real-time experimentation and recording system REX (Hays et al. 1982) received the data online from the Zebris device, the force sensor, and the contact signal and mapped all these data in a common sampling frame (1 kHz). This system provided the real-time control signals to trigger the magnetic brake and to open and close the shutter glasses.

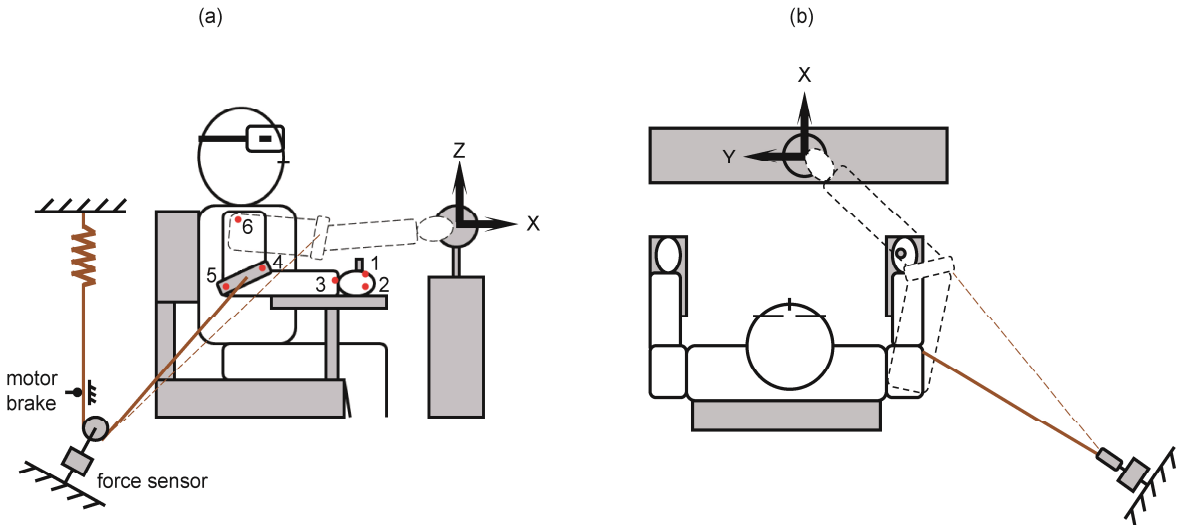

Figure 2.1: *Experimental setup. (a): Side view. The order of markers 1-6 was as follows: basal joint of index finger; basal joint of little finger; center of wrist; medial above the elbow; lateral above the elbow; and acromion. (b): Top view. The solid arm shows the start position and the dashed arm shows the end position. The world fixed coordinates [X, Y and Z] were illustrated.*

Procedure

At the beginning of each trial, the subject was instructed to bring the dominant right hand to the start position (in which the hand grasped the handle on the chair, as seen in Fig. 2.1 the solid-drawn arm). The subject pressed a button with the left hand to indicate being prepared for the movement. After a random delay of between 1.3 and 2.3 s a beep served as a go-signal, and the subject reached for the target in a natural way without any particular

speed requirements and grasped the metal ball with a power grip which involved all digits. The shutter glasses closed at movement onset, which was defined as the time when the tangential velocity of the first marker (marker 1 in Fig. 2.1) exceeded 0.25m/s. The shutter glasses opened 2 s later, after the end position of the hand was reached. Then the subject returned the hand to the start position naturally and prepared for the next trial. Each subject performed 100 trials of reaching movement consisting of two trial types: unperturbed and perturbed trials. During 20% of all trials an impulse-like perturbation was triggered when the position signal of the first hand marker exceeded 60% of the distance between the start position and the target. The time point when the marker crossed this threshold was used to elicit the digital command for the magnetic brake. Post-hoc analysis of the recorded force signal showed that, because of the mechanical delay of the brake, the perturbation onset occurred 16 ms later. This point in time is referred to hereafter as "perturbation onset" or "trigger time". These perturbed trials were randomly interspersed among the unperturbed trials. Offline analysis showed that at trigger time the standard deviation of all joint angles across trials was small and stayed in the range of 1.7 to 4.9 deg.

The perturbation was brief and small. The peak force amplitude was about 7-16 N. It was reached 150 ms after the hand position trigger and decreased to about 10% of peak force 210 ms after this trigger. During unperturbed reaching movements, the rope could move smoothly and the preloads induced by the low-stiffness spring stayed below 2 N. The preload force and the perturbation force for a sample subject are shown in Fig. 2.2.

Data Analysis

Kinematic analysis

(1) Movement duration, hand velocity, hand cumulative path length and hand end position

To quantify the general characteristics of the whole movement, some dependent variables were of interest. Movement duration was defined as the time interval between the movement start (200 ms before the motion of the first hand marker was detected) and the movement end (the first contact with the target). The tangential hand velocity was computed as the tangential velocity of the first marker position (world fixed coordinates, see Fig. 2.1). The hand cumulative path length was defined as the sum of the distances

between all successive sampling points along the trajectory. Hand end position was defined as the position of the first marker at movement end in world fixed coordinates.

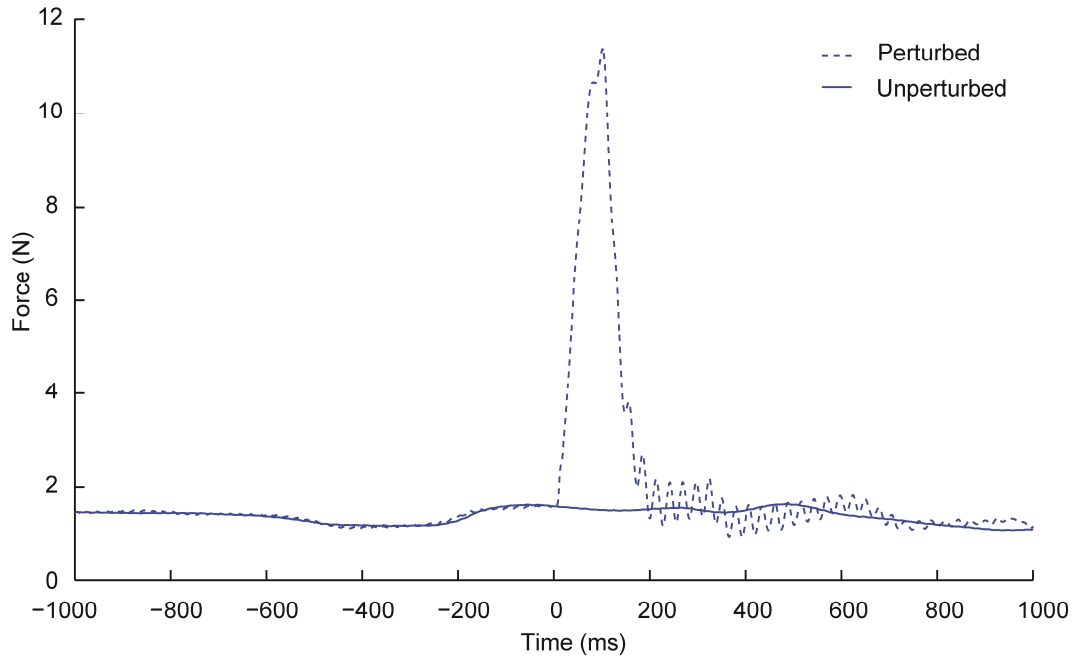

Figure 2.2: *Force exerted by the rope for one subject averaged across 14 perturbed and 58 unperturbed trials. Time 0 indicates the perturbation onset.*

(2) Joint angle and joint velocity

The seven joint angles of the arm, expressed as seven consecutive Cardan angles, were reconstructed from the 18 marker position signals (6×3). The order of joint angles was as follows: two angles for the wrist (vertical [WV], and horizontal [WH]), two angles for the elbow (torsion [ET], and flexion [EF]), and three angles for the shoulder (torsion [ST], horizontal [SH], and vertical [SV]). The zero position of the arm was defined as the arm pointing straight forward, with the elbow extended and the palm facing up. Positive joint angle indicated the following directions: flexion or vertical upward, horizontal rightward, and torsion clockwise.

The time courses of joint angles were first interpolated in 1 kHz and then filtered by a symmetric (zero-phase) Gaussian low-pass with a cut-off frequency of 5 Hz (gain 0.04 at the Nyquist frequency of 15 Hz). A three-point differentiator was applied to obtain joint velocities. Joint end position was defined as the position vector of seven joint angles at movement end.

(3) Trace normalization

For every subject, an outlier analysis was performed separately for both trial types. Trials with movement durations that were more than 3 standard deviations from the mean of the respective trial type were excluded as outliers. Then, by interpolation, the movement durations of all trials were normalized to the average movement duration of the respective group. Then, also trials were eliminated as outliers if any of the seven joint angles at any time during the movement was more than 3 standard deviations away from the mean of the respective joint angle at that time across all trials of the corresponding type. On average 4 perturbed trials out of 20 and 24 unperturbed trials out of 80 were excluded.

Dynamic analysis

The dynamic arm model had three segments: the hand was modeled as a ball, while the forearm and upper arm were modeled as two frustums. The geometry, mass and inertia of the three arm segments for each subject were determined using anthropometric data (Winter 2009) and measurements of the individual length of the subject's upper arm, forearm, and hand (calculated from the recorded marker positions) and the subject's weight and height.

The three-segment arm dynamics of seven DoFs were modeled by the following nonlinear differential equation:

$$\frac{d}{dt}\frac{\delta L}{\delta \underline{\dot{q}}} - \frac{\delta L}{\delta \underline{q}} = \underline{\tau}_{in} + \underline{\tau}_{ext} \tag{2.1}$$

equivalent with

$$\frac{\delta^2 L(\underline{q},\underline{\dot{q}})}{\delta \underline{\dot{q}}^2}\cdot\underline{\ddot{q}}+\frac{\delta^2 L(\underline{q},\underline{\dot{q}})}{\delta \underline{\dot{q}}\cdot\delta \underline{q}}\cdot\underline{\dot{q}}-\frac{\delta L(\underline{q},\underline{\dot{q}})}{\delta \underline{q}}=\underline{\tau}_{in}+\underline{\tau}_{ext} \tag{2.2}$$

The left side of the equation denotes the arm dynamics in the Lagrange form. Here, L is the Lagrange function which is defined as the difference between kinetic energy ($E_{kin}(\underline{q},\underline{\dot{q}})$) and potential energy ($E_{pot}(\underline{q})$) of the arm system. The potential energy included only energy related to displacements of the mass in the field of gravity but no viscoelastic components. $\underline{q}$ and $\underline{\dot{q}}$ denote the joint angle vector and velocity vector, with seven DoFs. The variables on the right side of the equation denote the joint torques. $\underline{\tau}_{in}$ is the joint torque caused by muscle torques and $\underline{\tau}_{ext}$ is the joint torque equivalent to the applied external forces ($\underline{f}$). Note that the muscle torques comprise passive (viscoelastic) and active components which were not further distinguished by the mechanical model. External torques were computed according to Khatib (1987)

$$\underline{\tau}_{ext}=\left(\frac{d\,\underline{x}_e(\underline{q})}{d\,\underline{q}}\right)^T\cdot\underline{f} \tag{2.3}$$

where $\underline{x}_e$ denotes the position of the elbow joint, $\frac{d\,\underline{x}_e(\underline{q})}{d\,\underline{q}}$ its Jacobian matrix with respect to the joint angles $\underline{q}$, and $\underline{f}$ the force vector pointing in the direction of the rope.

Providing the arm model mechanical structural parameters, the arm kinematics, and the external perturbation $\underline{\tau}_{ext}$, Equation 2.1 was evaluated for each sample to obtain the muscle torque $\underline{\tau}_{in}$ for every valid trial of each subject and for each trial type. We assumed the muscle torque to be separable into two components, one proportional to gravity and the other independent of it (Gottlieb et al. 1997). The gravitational component was computed by:

$$\underline{\tau}_g=\frac{d\,E_{pot}(\underline{q})}{d\,\underline{q}} \tag{2.4}$$

For joint torque analysis, the gravitational torque was removed and the residual was defined as "dynamic" torque:

$$\underline{\tau}_d = \underline{\tau}_{in} - \underline{\tau}_g \tag{2.5}$$

To test the correctness of the inverse dynamic computation we numerically integrated the dynamic system (Eq. 2.2) and verified that the resulting simulated trajectory was identical with the measured one.

Evaluation of the perturbation response

For each subject, all valid trajectories of joint angles and joint torques for both trial types (perturbed and unperturbed) were temporally aligned at the trigger time, which was defined as time zero. The following dependent variables were used to illustrate the perturbation response:

(1) $\underline{\tilde{q}}$: Joint angular difference between perturbed and unperturbed trials. This variable quantifies the perturbation-induced displacement of the arm and is called *joint displacement* hereafter.

(2) $\underline{\tilde{\tau}}_{resp}$: Dynamic torque (i.e. $\underline{\tau}_d$ in Eq. 2.5) differences between perturbed and unperturbed trials. This variable quantifies the joint torque response of the subject and is called *torque response* hereafter.

(3) $\underline{\tilde{\tau}}_{ext}$: External force perturbation mapped to joint space. This variable, called *perturbation torque* hereafter, quantifies the joint torque that would have to be compensated by the subject in order to avoid any perturbation-induced displacement. It was computed as the difference of the external torque (i.e. $\underline{\tau}_{ext}$ in Eq. 2.3) between perturbed and unperturbed trials

Since the perturbation force was exerted on the elbow joint, the evoked external torques acted exclusively in the horizontal and vertical shoulder angles. From Equation 2.3 it can be easily derived that the external torques in other joint angles were zero.

The onsets of joint displacement and torque response for the shoulder joint were detected as follows: For each sample within a time window of ±200 ms around the trigger time, Hotelling's two sample t-test was performed on the difference between perturbed and unperturbed trials. The onset time was defined as the latest time point where the two means did not differ at a level of $p>0.05$.

To determine the relative orientation of joint displacement, torque response and perturbation torque in the shoulder joint, a principal component analysis was performed on each of the respective 3D-trajectory. All samples from a time interval of 300 ms after perturbation onset were included. The first of the resulting eigenvectors defined the main direction of these trajectories. The relative orientation of pairs of these trajectories was evaluated by the angle between the corresponding first eigenvectors. Same or opposite directions are indicated by 0 or 180 deg respectively.

2.3 Results

Movement kinematics

Movement duration and hand cumulative path length

For unperturbed trials, the mean movement duration was 833±96 ms. The perturbation affected the mean movement duration (paired t-test: $t(9)=-3.7$, $p<0.005$, Fig. 2.3a), which was on average 112 ms longer for the perturbed than for the unperturbed trials, but not the standard deviation across trials of movement duration ($t(9)=-1.1$, $p>0.3$).

The mean hand cumulative path length was 0.360±0.024 m for unperturbed trials and did not depend on trial types ($t(9)=-1.5$, $p>0.16$, Fig. 2.3b). The perturbation did not have an effect on cross-trial standard deviation of hand cumulative path length ($t(9)=-0.4$, $p>0.7$). These results indicated that the perturbation caused a transient effect on the hand velocity but not on the hand trajectory.

Hand end position and joint end position

For unperturbed trials, the mean hand end position (coordinate [X, Y, Z] in Fig. 2.1) was [-75 ± 15 mm, -25 ± 12 mm, 34 ± 10mm]. Paired t-test showed that hand end position did not differ between perturbed and unperturbed trials (for all three coordinates: $t(9)<1.7$, $p>0.13$), see Fig. 2.3c.

The joint end positions [ST, SH, SV, ET, EF, EV, EH] for unperturbed trials were [-47.4 ± 2.9 deg, 16.6 ± 2.3 deg, -21.6 ± 3.1 deg, -87.2 ± 4.8 deg, 42.4 ± 5.0 deg, -11.1 ± 3.1 deg, -3.3 ± 2.0 deg]. Compared with perturbed trials, the shoulder torsion angle ($t(9)=5.94$, $p<0.001$) and wrist horizontal angle ($t(9)=-3.07$, $p<0.02$) were affected, but the other joint angles were not ($-2.25<t(9)<1.68$, $p>0.05$), see Fig. 2.3d.

Hand velocity and joint angular velocity

To show the complexity of the unperturbed reaching movement, hand and joint velocity profiles of a sample subject are presented in Fig. 2.4. The hand movement was fairly straight with a bell-shaped velocity profile (Fig. 4a). The velocity curve of vertical

shoulder angle was also bell-shaped (Fig. 2.4d), while shoulder torsion, horizontal shoulder angle and elbow flexion possessed biphasic velocity profiles (Fig. 2.4b, c and f). The velocity curves for elbow torsion, horizontal wrist angle and vertical wrist angle (Fig. 2.4e, g and h) were relatively smooth before the contact (dashed line in Fig. 2.4). For wrist movement there was a pulse in the velocity profile immediately after the first contact (Fig. 2.4g, h, after the dashed line), induced by the contact of the hand and the target.

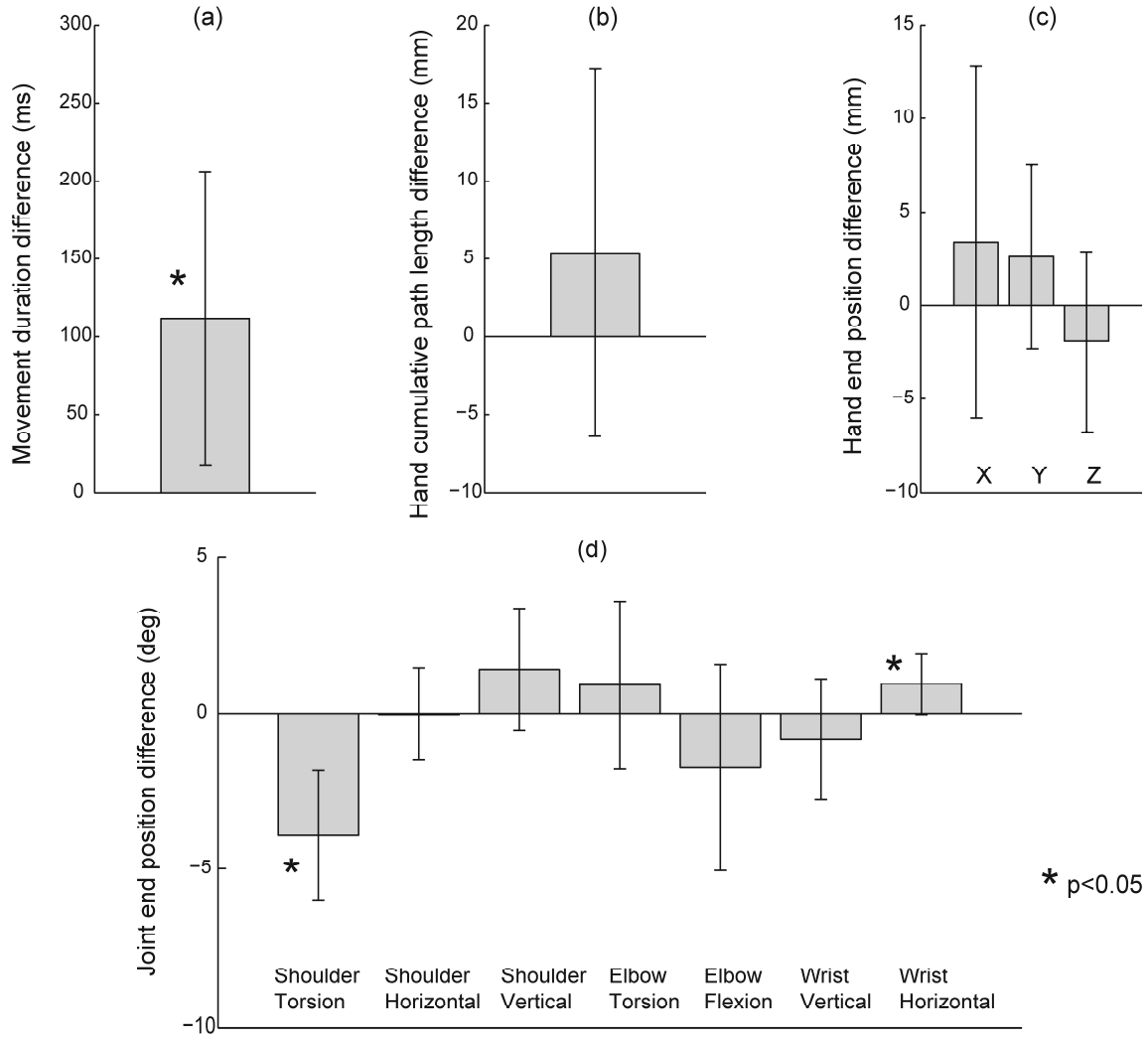

Figure 2.3: *Paired difference (perturbed – unperturbed) of movement duration (a), hand cumulative path length (b), hand end position (c) and joint end position (d). The error bars represent standard deviation across subjects. Asterisks indicate statistical significance $p < 0.05$.*

The similarity of the bell-shaped velocities of the hand and vertical shoulder angle, as well as the biphasic velocities of shoulder torsion, horizontal shoulder angle and elbow flexion, was consistent in all subjects. However, the velocity curves for elbow torsion, vertical wrist angle and horizontal wrist angle before the contact were quite different among subjects (e.g. the same joint angles could show single peak, multiple peaks or irregular shapes in different subjects). The impulse-like wrist velocity profile after the first contact occurred in most of the subjects. The average hand peak velocity across subjects was 0.78 ± 0.16 m/s which occurred at 58.5% ± 8.3% of the movement duration. The vertical shoulder angle had a peak velocity of 143 ± 32 deg/s at 65.3% ± 6.4% of the movement duration.

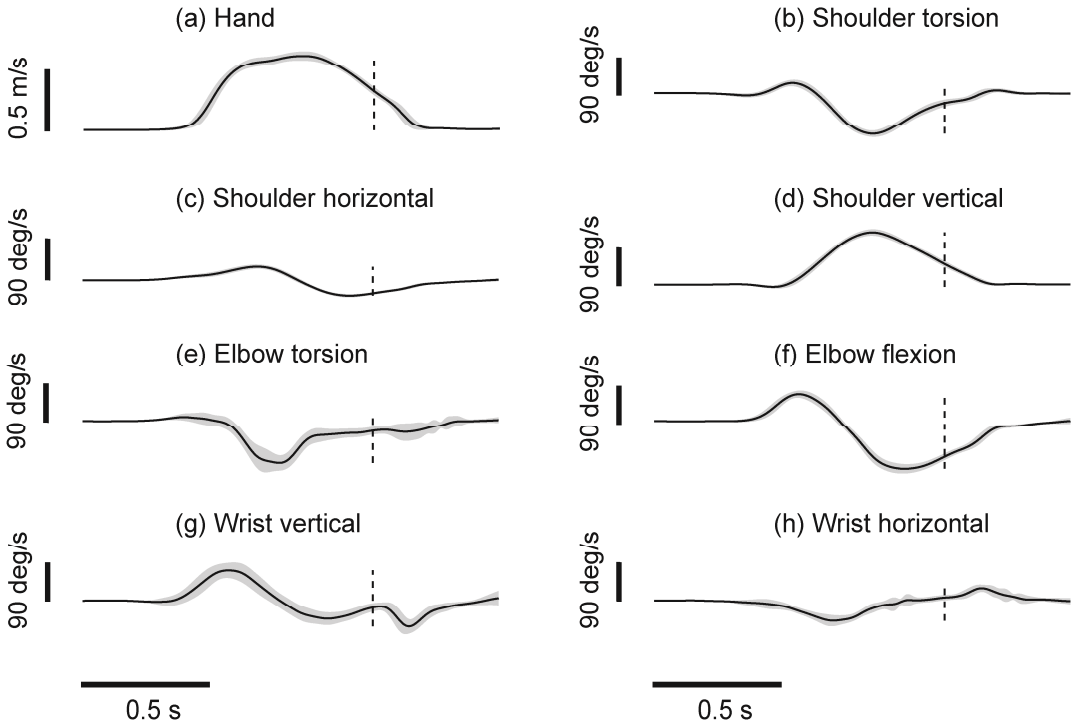

Figure 2.4: *Mean (±standard deviation) of hand velocity (a) evaluated as the tangential velocity of marker 1, and joint velocities (b-h) for one subject, averaged across 60 unperturbed trials. The dashed vertical line indicates movement end (the first contact with target).*

Dynamic torques

Fig. 2.5 illustrates the seven joint dynamic torques (after removing the gravitational component from the generated muscle torques) of unperturbed reaching movement for one subject. Note that in Fig. 2.5 the joint angles have different torque scales and the time interval ends at the contact with the target. Biphasic torque profiles were observed in most joint angles, e.g. horizontal shoulder angle (Fig. 2.5b), elbow flexion (Fig. 2.5e) and horizontal wrist angle (Fig. 2.5g). The vertical shoulder angle (Fig. 2.5c) had a near biphasic torque waveform, with the largest peak-to-peak amplitude (3.5 Nm) compared to other joints. The dynamic torque profile of elbow torsion (Fig. 2.5d) had multiple (>2) peaks.

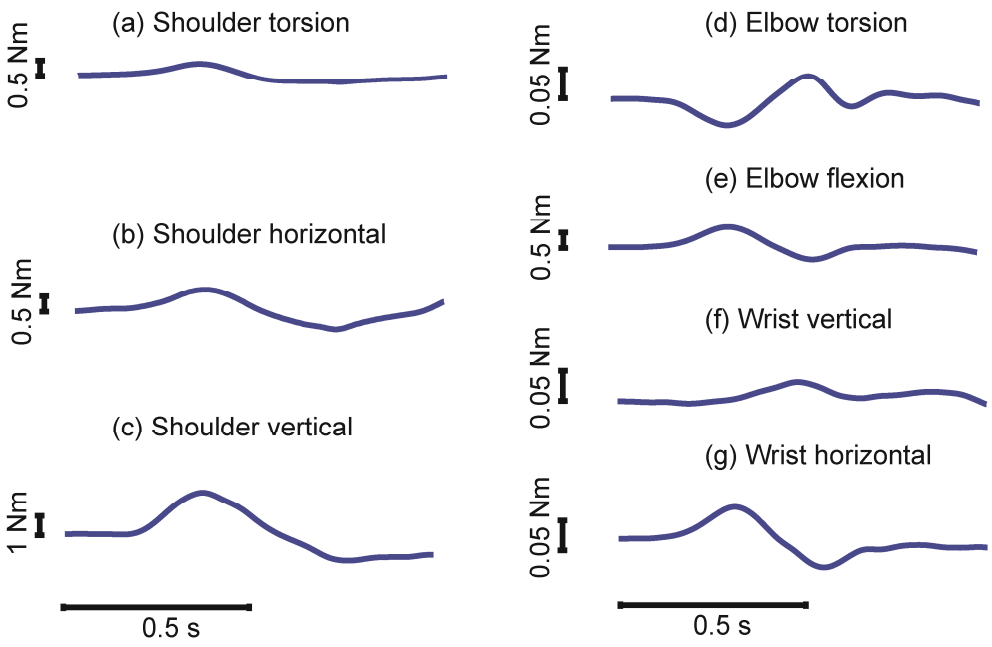

Figure 2.5: *Dynamic torques of seven joint angles for the same subject as shown in Fig. 2.4 during unperturbed reaching movement. Note that the torque scales differ across joint angles.*

The torque profiles of vertical shoulder, elbow flexion, and horizontal wrist joint (Fig. 2.5c, e and g) as well as shoulder torsion and elbow torsion (Fig. 2.5a and d) were consistent among all subjects. In contrast, horizontal shoulder and vertical wrist torque profiles varied largely among subjects.

Perturbation response

Fig. 2.6 shows the joint displacement, torque response and perturbation torque of all three shoulder joint angles in one subject. For all 10 subjects the largest torque responses were observed in the horizontal and the vertical components of the shoulder joint, with opposite signs to perturbation torques. The average joint displacement started at 86±25 ms, significantly (paired t-test: $t(9)=11.0$, $p<0.001$) later than perturbation onset of the perturbation torque (0 ms). The mean onset time of torque response was 62±38 ms and also differed from zero ($t(9)=5.1$, $p<0.001$). The onset time of joint displacement and torque response did not differ (paired t-test: mean difference=24±42 ms; $t(9)=1.8$, $p>0.1$).

The peak absolute torque response and perturbation torque were 3.1±1.4 Nm and 2.6±0.7 Nm respectively. The peak of absolute torque response occurred 193±59 ms after the onset of the perturbation torque and was 120±12 ms after the peak of absolute perturbation torque ($t(9)=3.6$; $p<0.01$). With the exception of the vertical shoulder displacement, which was relatively small in all subjects, the number, sign, and relative size of the peaks of joint displacements and torque responses in Fig. 2.6 were consistent across all subjects.

The principal component analysis of joint displacement and torque response revealed that their directions were concentrated around the first eigenvector which explained 92.9±8.3% and 85.6±9.6% of their respective total variance. Unsurprisingly, since changes in the joint angles during the perturbation were small, the first eigenvector of perturbation torque accounted for more than 99% of its variance. The relative orientation of joint displacement, torque response and perturbation torques in the shoulder joint showed that the direction of the torque response was almost opposite (161.7±11.6 deg) to that of perturbation torque. Joint displacement was far from being collinear with torque response (88.2±31.8 deg) or with perturbation torque (92.6±35.9 deg) due to large torsional components in the displacement (Fig. 2.6a).

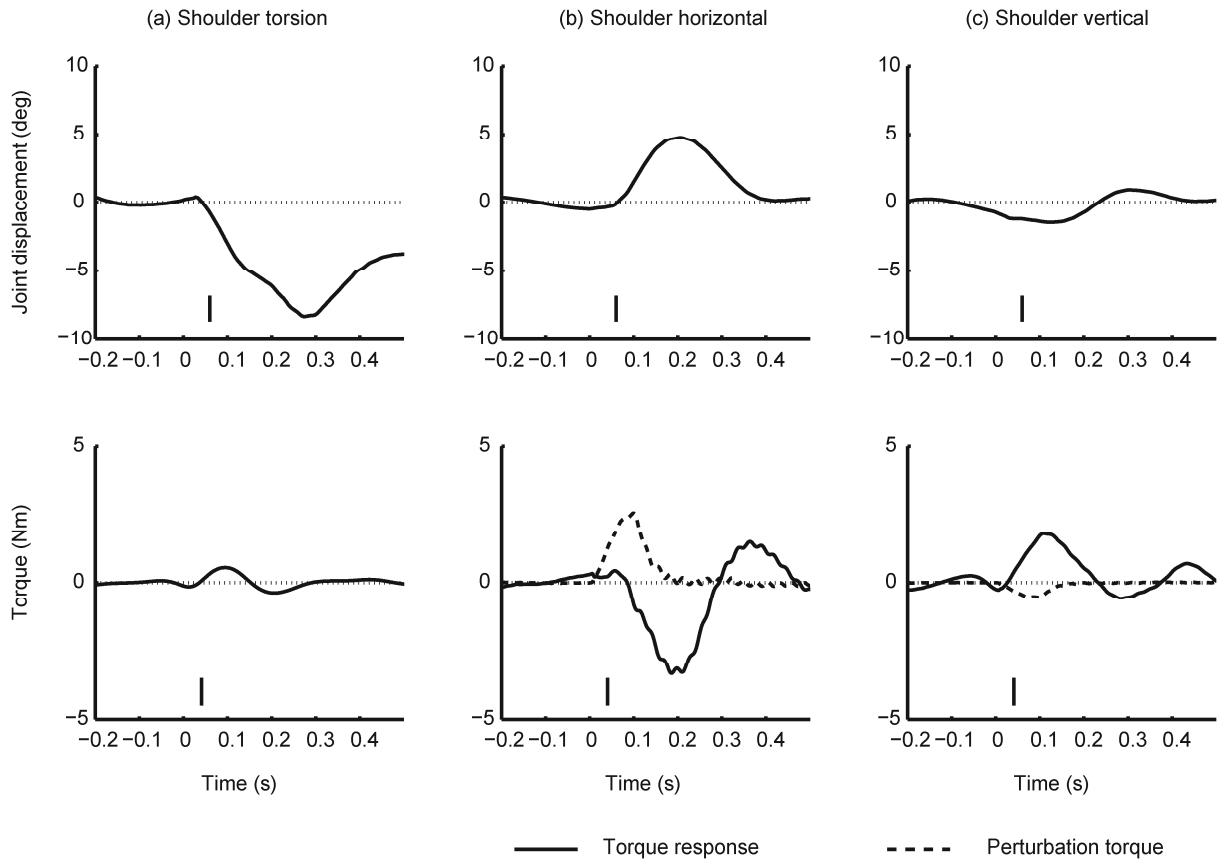

Figure 2.6: *Typical patterns of joint displacement and torque response of the three shoulder joint angles in one sample subject. The mean joint displacement (top, solid lines) and torque response of each joint angle (bottom, solid lines) are shown, starting from 200 ms before trigger time (Time=0). The dashed lines, in the lower row of (b) and (c) indicate the mean perturbation torque. The small vertical marks indicate the onsets of joint displacement or torque response.*

2.4 Discussion

The present study demonstrated the kinematic and dynamic characteristics of the full DoF reaching movement. The hand tangential velocity was quite similar to that in 2D reaching while joint kinematics and dynamics showed more complex profiles than in 2D planar movements. Using a simple perturbation apparatus, torque responses to external impulse-like perturbation during full DoF reaching were quantified. The onset of torque response was almost simultaneous with the onset of joint displacement. The torque response was mainly observed in the same joint angles as external perturbation torques, with time profiles of similar shapes but opposite signs for each joint angle. In contrast joint displacement and torque response were far from being collinear.

Kinematics and dynamics of unperturbed 2D and 3D reaching

In this section we discuss which characteristics of 2D movement control also apply to reaching movements with full DoFs.

The hand movement characteristics in this experiment (Fig. 2.4a) were similar to those of 2D planar reaching movements (Morasso 1981; Flash and Hogan 1985), reaching in the sagittal plane (Lacquaniti and Soechting 1982; Atkeson and Hollerbach 1985) as well as 3D reaching with full DoFs (Mattos 2011). In these studies, like in the current study, the hand movement distance was about 30 ~ 50 cm and movement duration was 0.8 ~ 1 s. The hand profile of the tangential velocity was bell-shaped with a maximum of approximately 0.8 to 1.5 m/s. Hand trajectory was smooth and nearly straight. The similarity in hand kinematics between movements underlying different constraints suggests that the bell-shaped hand kinematics are an essential part of the movement plan (Morasso 1981; Flash and Hogan 1985) which is quite independent of partial constraint.

The multiple velocity peaks of some joint angles (Fig. 2.4b-h) in the current study indicate the increased complexity of the dynamic system compared to 2D movements. The increase in complexity is also reflected by the torque profiles which were non-biphasic in some joint angles (Fig. 2.5d and f). Elbow torsion and vertical wrist angle showed high variability of joint velocity (Fig. 2.4e and g). Large inter-trial variability of the elbow torsion was also observed by (Krüger et al. 2012) and suggests that stabilization of this

joint torque is of minor importance in movement control, possibly because it has only a small effect on hand position. The initial peak in the biphasic velocity profiles of shoulder torsion, horizontal shoulder angle and elbow flexion (Fig. 2.4b, c, and f) were likely due to the mechanical constraint at the movement start where subjects needed to move the hand aside from the initially grasped handle.

In the presence of high redundancy, such as the full DoF reaching in our case, one important question is how the motor system reduces the number of DoFs to simplify the control strategy. One possibility is to introduce a strong correlation between DoFs, limiting the high dimensional motor space to a lower dimensional subspace, i.e. motor primitive or synergy (Bernstein 1967). This idea has been extensively studied at various levels of analysis: kinematics (Pozzo 2002; Lee 2008; Berret 2009; Grimme et al. 2012; Schütz and Schack 2013), dynamics (Grinyagin 2005; Thomas 2005) and muscle activation (Soechting and Lacquaniti 1989; d'Avella 2006; Tolambiya 2011). The spatiotemporal organization of the muscle patterns for various types of movements, e.g. from multi-joint arm reaching (d'Avella 2006) to whole body pointing (Tolambiya 2011), can be characterized by the coordinated activation of muscle groups, or time-varying muscle synergies. Only 4 or 5 combined explained about 75% of the data variation. For the unperturbed movements in our experiment, a principal component analysis of the time courses of joint angles and joint torques showed that the first eigenvector explained 89.7±3.9% and 83.5±7.4% of their respective total variance. This suggests that motor synergies also played an important role in the current experiment. However, further experiments with varying end points are necessary to verify that the observed synergies also apply to movements with different end points.

In summary, our observation showed complex kinematic and dynamic movement patterns in unconstrained reaching movements. However, many aspects of these patterns were also observed in 2D movements such as bell-shaped hand velocity and the biphasic torque profiles in certain joints. The common aspects suggest similarities in the objectives of the underlying movement plans.

How well do torque responses compensate for the perturbation?

Active muscle force

Insightfully, a few previous perturbation studies (both during posture and movement) showed that the early EMG response to perturbation started less than 40 ms after perturbation onset, and the main part of the later EMG response was counteracting perturbation (Lacquaniti and Soechting 1984, Lacquaniti and Soechting 1986a, Lacquaniti and Soechting 1986b, Soechting and Lacquaniti 1988, Soechting 1988). These experiments were performed during 2 DoF movements. In this study, we extended the approaches to full 7 DoF reaching movements and applied perturbations to the elbow joint. In our experiment the initial torque responses had a latency of 60 ms after perturbation onset, while in the studies of Soechting and Lacquaniti as well as other studies (Smeets et al. 1995; Kurtzer et al. 2008), onset latencies of early EMG responses were in the range of 20-45 ms after perturbation onset. The later onset of torque responses than EMG responses could be due to the electromechanical delay in human skeletal muscles (Norman and Komi 1979). Our results showed that peak torque response occurred about 200 ms after perturbation onset. This timing is about 100 ms later than the peak of EMG response observed in shoulder muscles during impulse-like force perturbations in 2D arm movements (Lacquaniti and Soechting 1986a, Lacquaniti and Soechting 1986b, Soechting 1988, Soechting and Lacquaniti 1988). This discrepancy may be due to the perturbation duration which was 40-50 ms in these studies and thus only about 25% of the perturbation duration of the current study.

Passive muscle force

At very short latency, torque responses to external perturbation may be related not only to active muscle force (as indicated by EMG measurements), but also to passive, viscoelastic muscle forces. Torque generated by muscle stiffness has a very small time delay (<1 ms) as shown by Cecchi et al. (1986) who measured changes of muscle tension induced by a sudden change of muscle length. These forces can react almost instantaneously to a change of muscle length and can contribute to the observed early torque responses in our experiment. Forces related to viscous forces could explain torque responses starting before

joint displacement, which seemed to be the case for some of our subjects, even though this was not significant for the group mean.

Relative orientation of torque responses

Our experiment provides an example in which the main direction of the torque response contributes to the stabilization of unconstrained arm movements. Our results showed that torque responses were mainly elicited in the same joints where perturbation torques applied, see Fig. 2.6b and c, and it further suggested that the main components of the shoulder torque responses were compensatory, i.e. were opposite to perturbation torques. The first eigenvector of the torque response accounted only for 85% of its total variance, suggesting that the early (t=80 ms) components of the torque response did not align with its main component. Fig. 2.6a shows that the early torque response, in contrast to the perturbation torque, contained small torsional components. This direction difference between early and late torque response is compatible with observations that early and late EMG responses can have opposite signs (Soechting and Lacquaniti 1988; Smeets et al. 1995) and that in many cases the early response may actually assist rather than compensate the perturbation (Hasan 2005).

In contrast, the main components of joint displacement were not collinear to the perturbation torque. Fig. 2.6a shows a large displacement of shoulder torsion which did not have a counterpart in the torque response or in the perturbation torque. This is a consequence of the nonlinear dynamics of the 7DoF arm as confirmed by simulating the joint displacement resulting from the perturbation torque (Fig. 2.6b and c, dashed) in the absence of any torque response. In this simulation with the described dynamic model (Equ. 2.2) the displacement of shoulder torsion and horizontal wrist reacted most sensitively and reached a value of 1 deg at a latency of 46 ms after perturbation onset, which was similar to the experimental data (Fig. 2.6a). The simulated horizontal displacement reached a value of 5 deg at a latency of 90 ms after perturbation onset, which was much earlier than the experimental data. Thus, the horizontal shoulder angle was more efficiently stabilized by the torque response than shoulder torsion.

Absence of adaptive changes of movement control

A further question is whether the observed short-latency response was specifically adapted to the particular perturbation applied during this experiment. To address this question we repeated the same computation of the torque response separately for the first and the second half of the data of each subject. Neither the response delay ($t(9)=0.10$, $p=0.92$) nor the peak of the absolute torque response ($t(9)=1.34$, $p=0.21$) differed between the first and the second half. This suggested that our response was not subject to an adaptive process.

This absence of adaptive adjustments concerned both feedforward and feedback control and was probably due to two particular features of our experimental setup: First, torque perturbations were small enough to be sufficiently compensated and thus to have little effect on hand end position during relatively large movements (Sanes and Evarts 1983). Therefore, there was only very limited need for adaptation. Second, perturbations were only applied rarely (20%) and were randomly interspersed with unperturbed trials. This condition is known to reduce adaptive changes compared to pure (100%) perturbation conditions (Fan et al. 2006; Wei et al. 2010).

Complexity of a feedback controller

Another interesting question is whether the observed torque response in our experiment can be generated by a reflexive control mechanism that effectively implements an internal dynamic model of the arm (Kawato 1999). Such a capability would be unexpected for a short latency reflex since it was shown that, e.g., the short-latency reflexes of the shoulder muscles were linked exclusively to the movements of the shoulder and not to the movements of other joints (Kurzer et al. 2008). In order to implement a full dynamic model of the arm, the interaction between different joints would have to be considered as well. This seems only to be possible for long-latency reflexes (Kimura et al. 2006; Kurzer et al. 2008). To explain our response it is not necessary to assume the involvement of a full dynamic internal model of the arm since our perturbation as well as the observed response concerned mainly shoulder torques.

2.5 Conclusions

The current experimental setup and the analysis methods were shown to be suitable for analyzing joint torques in unconstrained reaching movements with full DoFs. Furthermore, the method allowed short-latency perturbation responses in these complex movements to be quantified. Even though joint angle and velocity profiles were more complex than arm movements constrained to 2D in some aspects, the bell-shaped profile of tangential hand velocity seems to be an essential part of the movement plan for constrained and for unconstrained movements. Early torque responses to perturbations were likely to be a combination of viscoelastic muscle properties and short-latency reflexes. The main components of torque responses were opposite to perturbation torque, while this did not hold as strictly for the very early components of the torque responses. Torque responses did compensate for hand displacement at movement end, but early after perturbation onset not all dimensions of the joint displacements were stabilized with equal efficiency.

Acknowledgements

We gratefully thank Katie Ogston for proof-reading the manuscript. This work was supported by the Research Training Group 1091 “Orientation and Motion in Space” of the Germany Research Foundation (DFG).

3. Peripheral Mechanisms Compensate Efficiently for Small Perturbations[1]

Abstract

Unexpected external perturbations during reaching movements are normally compensated for automatically and unconsciously. Previous studies observed that, in the case of transient small perturbations, the motor system was able to converge to the preplanned end position. The question is whether supra-spinal motor signals are actively involved in this compensation or whether the peripheral control mechanisms formed by intrinsic muscle properties and the stretch reflex are sufficient. This is suggested by a model (Pilon and Feldman 2006) explaining the movement dynamics by peripheral mechanisms responding to a shift of reflex parameters, which are in turn provoked by descending control commands which settle early during the movement. The present study tests how efficiently such peripheral mechanisms can account for the compensation process during single-joint fast reaching. Motor responses to transient small perturbations at different movement phases were measured and compared with the predictions of the model. The results show good agreement concerning kinematic and dynamic responses. Significant responses of joint torque and electromyographic activity were observed already 50 ms after perturbation onset. The perturbation-induced displacement was reduced to 40% of its peak value within 100 ms, demonstrating the efficiency of fast motor responses. Simulation results with altered mechanical parameters of the model suggest that reflexive responses are well tuned to the intrinsic muscle properties and both probably play an important role in movement stabilization. We conclude that the stretch reflex loop and intrinsic muscle properties cope efficiently with small transient perturbations.

[1] Adapted from Zhang L, Straube A, Eggert T (2014) submitted

3.1 Introduction

The human motor system is a complex biological control system that can perform goal-directed tasks, such as reaching. These reaching movements can be performed precisely even under unexpected external interference. For example, during a goal-directed reaching movement, it reacts to an external mechanical perturbation by generating a motor response. In order to achieve the behavioral goal successfully, such a motor response has to be compensative, i.e. it helps to minimize the consequence of the perturbation. The motor system can generate fast compensation (latency < 50 ms) only by means of peripheral and spinal mechanisms while transcortical loops have longer latencies. Rapid peripheral control mechanisms comprise both passive and active components. The passive component with almost zero delay is generated due to the intrinsic mechanical properties of active muscles (Cecchi et al. 1986, Krylow and Rymer 1997). In response to a deformation, the muscle generates force which is both length- and velocity-dependent. These intrinsic properties are called elasticity and viscosity respectively (Fung 1993). The active component is produced by the spinal stretch reflex, which regulates the muscle activity with a time delay of about 20-45ms (Pierrot-Deseilligny and Burke 2005). For later responses (>50 ms), a supra-spinal response, which is usually called a long-latency response, may take effect (Lee and Tatton 1982, Lewis et al. 2005) and later (>100 ms) an intentional response may follow.

Especially the short latency motor responses reflect feedback mechanisms which highlight the role of proprioceptive sensory feedback in motor control. When perturbation is transient and small the system can reach the same final position (Schmidt and McGown 1980, Rothwell et al. 1982, Jaric et al. 1999). Short transient responses are likely to be dominated by peripheral mechanisms such as the spinal reflex and passive responses, since supra-spinal control is too slow. A detailed model of how the stretch reflex acts during the movement was provided by Feldman and Levin (1995). Fast movements are generated by descending commands inducing a rapid shift of the threshold parameters determining the proprioceptive reflexes. Such a shift precedes the initial agonist EMG activity (Feldman and Levin 1995). The model of Feldman and Levin (1995) captures essential features of the physiology of the peripheral neural control. Even though there is ongoing debate about top-down control of the reflex sensitivity shortly before and in the very early phases of movement (Adamovich et al. 1997, Brown and Cooke 1981, Dietz et al. 1985, Shapiro et al.

2004, Niu et al. 2012), it is generally believed that reflex mechanisms are active during intermediate and later movement phases (Milner 1993, Bennett 1993, Latash 1994) and are mainly velocity driven (Smeets et al. 1990, Niu et al. 2010). In many other studies, similar experimental approaches using transient perturbations have been applied to measure arm mechanical parameters (Bennett et al. 1992, Burdet et al. 2000, Gomi and Kawato 1997 Popescu et al. 2003). However, it is not clear whether small transient perturbations that occur after the beginning of movement can be sufficiently compensated for by spinal reflex and passive responses. This is because the compensation of such perturbations takes much longer than 50 ms (Milner 1993, Bennett 1993, Latash 1994) and would theoretically allow central control loops to be involved.

The present study asks whether peripheral control mechanisms formed by the intrinsic muscle properties and stretch reflex are sufficient to compensate for small transient perturbations during fast movements, and to what extent, under such conditions, long-latency reflexes and other high-level control mechanisms have to interfere. To that purpose we measure motor responses to transient torque perturbations at different later movement phases and compare them with the predictions of a model proposed by Pilon and Feldman (2006). The onset and peak times of perturbation-induced displacement and displacement velocity, and the response torque, as well as the duration needed for 60% compensation are considered. Furthermore, the perturbation-induced EMG-response is also compared with the model prediction.

3.2 Methods

Subjects

6 subjects (4 males and 2 females, mean age: 34±10 years) participated in this study. They were all right-handed and were not suffering from any movement disorders. They were naïve with respect to the purpose of the study. The experimental procedure was in accordance with the Declaration of Helsinki and approved by the local Ethics Committee. Written consent was obtained prior to participation in the experiment.

Apparatus

The apparatus shown in Fig. 3.1 was used to investigate the arm response to external perturbations. The subject sat on a chair and the elbow joint was supported by a plate. The plate was about 1 m above the ground and mounted on the vertical rotary shaft of a ball bearing. The height of the chair was adjusted so that the subject's forearm could move in a horizontal plane passing through the shoulder. The elbow joint was aligned with the pivot and the forearm was fixed to the plate by a velcro tape. The location of the grasping handle on the metal bar for forearm support was adjusted to the forearm length. In the start position the elbow joint angle was flexed by about 60 degrees (full extension 0 degrees). A thin horizontal bar below the arm served as the target position at an elbow angle of 105 deg. Visual feedback during the movement was excluded by asking the subjects to close their eyes before movement started and open them again when movement ended.

Limb movement was recorded by a 3D ultrasound-based motion analysis device (Zebris Medical GmbH, Isny, Germany). One marker was attached to the grasping handle and was sampled at 200 Hz. The perturbation was applied by a high stiffness rope attached to the grasping handle. The pulling direction of the rope was in the horizontal plane where the subject moved the limb. The other end of the rope was connected with a low stiffness spring, which was fixed to the wall (Fig. 3.1b). The middle part of the rope went through a brake, where the rope could be suddenly jammed by a metal pin that could be pulled onto the rope by means of an electric magnet. The magnet was controlled by a digital signal switching the magnet on or off. When the magnet was switched off, the rope was released and could pass freely through the brake. The force in the rope was measured by a strain gage that allowed accurate dynamic force measurement (Rieger, Rheinmünster, Germany).

Surface EMG of the biceps and triceps was recorded by Neuropack (Soma Technology, Bloomfield, USA) with a built-in analog band-pass filter of 10-500 Hz. The amplifier has a gain of 10K, with input impedance > 200 mega-ohm. AgCl pre-gelled adhesive electrodes with a size of 20mmx25mm were used and the inter-electrode distance was 20mm. For the biceps, the electrode pair was attached at a central position over the muscle belly when the elbow was in the most flexed position. This helped to reduce the measurement error due to muscle migration below the electrode site during dynamic tasks. A neutral reference electrode was placed at the elbow bone area. The skin was cleaned with alcohol. The

impedance test showed that the resistance between the electrode pair was below 10 kOhm for all subjects.

A computer with a real-time experimentation and recording system REX (Hays et al. 1982) received the analog data online from the Zebris device, the EMG recording device and the force sensor, and mapped all these data in a common sampling frame (1 kHz). The resolution of the A/D measurement board was 16 bit with the amplitude range of +/- 10 Volts.

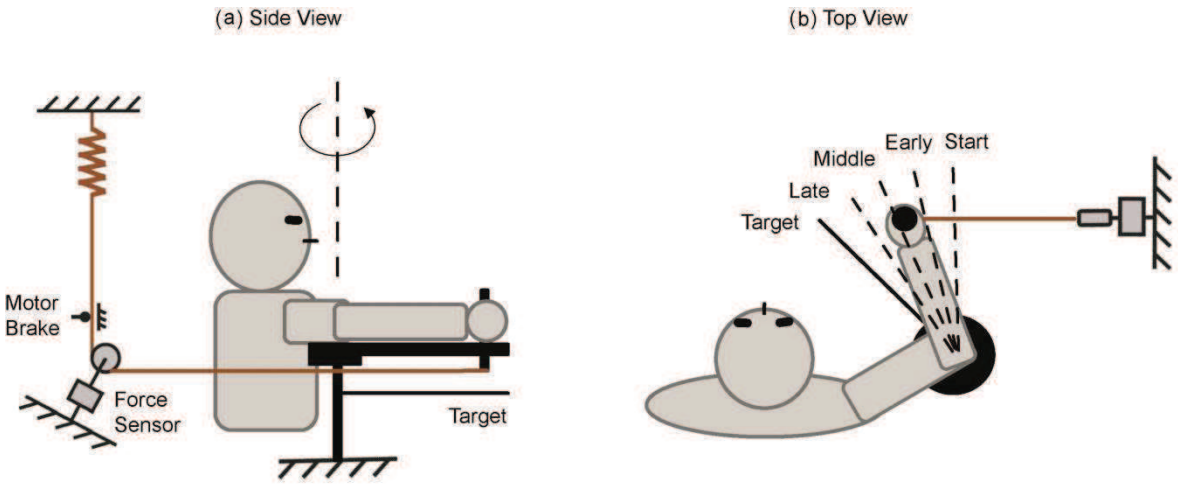

Figure 3.1: *Experimental Setup. (a) Side view. Elbow joint movement was recorded by an ultrasound marker placed on the top of grasping handle. The mechanism of the perturbation apparatus is described in the text. The pulling direction of the rope was to the right of the subject (see top view in (b)) and it was modified here in the side view for clarity. (b) Top view. Movement started at an elbow joint of 60 deg extension (full extension: 0 deg). The subject made a fast elbow flexion to the target (black solid bar), which was at the elbow position of 105 deg. An impulse-like perturbation could be triggered at an early (about 25%), middle (about 50%) or late (about 75%) stage of the movement.*

Procedure

Subjects were instructed to move the right arm from the start position to the target position in a single fast movement (45 deg elbow flexion). If the arm was perturbed during the movement, the subject was instructed to ignore the perturbation and not to correct in case the target was missed. Before each trial, the subject pressed a button to initiate the trial. A beep, generated at a random time interval between 1.3 and 2.3 s after the button press served as the go signal for movement initiation. Immediately after the beep the subject closed the eyes and initiated the movement. The subject's arm stayed at the movement end position until the eyes were opened. Then the subject returned to the start position and prepared for the next trial.

There were two trial types: unperturbed and perturbed trials. For perturbed trials, the magnetic brake was triggered when the position signal of the marker exceeded 25% (early), 50% (middle) or 75% (late) of the distance between the start position and the target, corresponding to about 25 ms before and 40 ms and 75 ms after the peak velocity. The duration of the braking was 100 ms and the corresponding torque perturbation along the movement direction was brief and small. Due to the velocity decrease, peak torque amplitude was systematically larger for the early and middle conditions (about 2.5-3 Nm) than for the late condition (about 2.2 Nm). For the early and middle trigger conditions, the perturbation torque reached its peak value about 80 ms after the hand position trigger and decreased to 10% of the peak about 150 ms after this trigger. For the late condition, the peak perturbation torque was reached about 40 ms after the hand position trigger and the perturbation torque decreased to 10% of its peak about 80 ms after this trigger. During unperturbed trials, the rope could move smoothly and the preloads induced by the low-stiffness spring stayed below 0.8 Nm.

Before the main experiment, each subject performed 30 practice trials (mixed trial types and trigger conditions, without vision during movement) to get familiar with the experiment. To allow a direct comparison of EMG results between subjects, all EMG responses were expressed as a fraction of the maximal voluntary contraction (MVC). MVCs were measured in a task in which subjects applied maximal isometric muscle force in the appropriate directions against the resistance of the experimenter.

The main experiment consisted of 150 trials in total, including 36 perturbed trials. Among all perturbed trials, each trigger condition (early, middle or late) had 12 trials which occurred in random order. The other 114 trials were unperturbed. All perturbed trials were randomly interspersed among the unperturbed trials. At least two consecutive unperturbed trials followed a perturbed trial, and later for the kinematic analysis, any unperturbed trial that appeared right after a perturbed trial was discarded to avoid any possible one-trial adaptation (Weeks et al. 1996). After this exclusion, 78 unperturbed trials were included in the analysis. After every 50 consecutive trials, the subject took a break for 5 minutes to prevent muscle fatigue.

Kinematic analysis

The elbow joint angle was reconstructed from the marker position. The zero position was defined as the configuration at the start position. The time course of the elbow joint angle was first interpolated in 1 kHz and then filtered by a symmetric (zero-phase) Gaussian low pass with a cut-off frequency of 30 Hz (transmission gain of 0.1 at 77 Hz). A three-point differentiator was subsequently applied to obtain elbow angular velocities.

For each trigger condition (early, middle, late), the position threshold for triggering perturbation was used to temporally align the perturbed trials with unperturbed trials. Movement start was defined as the time when velocity first reached 10% of its peak and movement end was defined as the time when velocity decreased to 10% of its peak. For every subject, an outlier analysis was performed separately for both trial types, based on the time interval between movement start and the peak velocity. Trials with a time interval that differed more than twice the interquartile range (25%-75%) from the mean of the respective trigger condition were excluded as outliers. On average about 1 perturbed trial out of 36 and 3 unperturbed trials out of 78 were excluded.

To quantify the consequence of the perturbation and how efficiently the motor system compensated for this effect, the joint displacement, defined as the position difference between perturbed and unperturbed trials, was analyzed in the time course. Displacement speed was defined as the velocity difference between two trial types (i.e. the derivative of displacement). The onsets of the displacement or the displacement speed were defined as the time when they first differed significantly from zero. To examine how efficiently the

motor system compensated for the perturbation effect we computed the time intervals between perturbation onset and peak displacement or the time when displacement decreased to 40% of its peak. These two time intervals were called the time of peak displacement and the time of 60% compensation respectively. By expressing both of the time points relative to perturbation onset, the timing of the compensation could be compared across trigger conditions. To quantify how well the perturbation effect was compensated for, we evaluated the displacement at 300 ms after the end of the unperturbed movements.

Limb dynamics

The dynamic model of the limb considers two segments: the hand was modeled as a ball and the forearm was modeled as a frustum. The inertia of the two limb segments for each subject was determined using anthropometric data (Winter 2009) based on the measurements of the subject's weight and height. The limb dynamics were computed by the following equation:

$$I\ddot{\theta} = \tau_m + \tau_{ext} \tag{3.1}$$

The total inertia I, including the inertia of the hand, the forearm, and the apparatus, was 0.098±0.024 kg·m²/rad. The elbow joint angle θ is 0 deg at the start position and increases when the elbow flexes. τ_m is the joint torque caused by muscle torques and τ_{ext} is the joint torque corresponding to the force that is externally applied by the rope.

Torque response was defined as the muscle torque (i.e. τ_m in Eq.3.1) difference between perturbed and unperturbed trials. Torque response onset was defined as the time when the positive torque response first differed significantly from 0.

EMG analysis

EMG signals captured from the A/D measurement board were digitally full-wave rectified, and then low-pass filtered with a two-way second-order Butterworth filter with 20 Hz cutoff frequency. Then MVC normalization was performed for each subject. The average

was taken in the time interval of 500 ms before and after the peak value of the rectified and filtered EMG signals during MVC task and used for MVC normalization. Thus all EMG potentials were expressed as a ratio relative to the maximum EMG potential.

EMG response was defined as the EMG difference between perturbed and unperturbed trials and its onset was determined by the following algorithm: for each muscle, the EMG values of two trial types were compared using the two-sample t test. The test was performed for each time sample to get a P value series. The EMG response onset was defined by the first significant difference of EMG values that lasted (i.e. P value remains < 0.05) for at least 20ms.

Model of threshold position control

According to the theory of threshold position control (Feldman 2011), the interaction between muscle fibers, muscle spindles, motoneurons, and the passive mechanics of the arm adjusts the joint angle to a desired position that is represented by a descending command called "the reference position" (R).

In this study, we used an implementation of the model of Pilon and Feldman (2006) who consider the case of one symmetric agonist-antagonist pair of muscles with a single joint (flexion/extension motion). In this model, two types of control commands are specified: the R command defines a joint angle, at which both muscles may be silent; the C command defines an angular range within which both muscles may be co-activated. Fig. 3.2a shows how the descending commands for the flexor ($\lambda_f = R+C$) and the extensor ($\lambda_e = R-C$) are defined by the combination of R and C. Here both of these descending commands are defined in units of joint angle (positive for elbow flexion). Fig. 3.2b shows how the command λ_f, modified by the muscle spindle feedback of the position θ and the velocity $\dot{\theta}$, determines the activation A_f of the flexor-motoneurons. λ_f^* is a dynamical signal integrating different inputs to the motoneurons (i.e. descending command, signals from reciprocal interneurons and velocity-dependent proprioceptive feedbacks). The muscle is activated (i.e. $A_f > 0$) only if λ_f^* exceeds the delayed position θ_d. The function of muscle torque generation in the static case is modeled by a nonlinear characteristic P_f, which is approximated by an exponential function, known as experimental invariant characteristics (Feldman and Orlovsky 1972). The gradual dynamic recruitment of the muscle torque M_f

is modelled as first-order low-pass with transfer function H(s). Surface EMG values were considered proportional to the static muscle torque P_f (St-Onge et al. 1997). Further negative feedback due to passive mechanics of the muscle (N, Q) modifies the muscle torque to explain the total flexor torque τ_f. The difference between flexor and extensor torques equals the total muscle torque ($\tau_m = \tau_f - \tau_e$). The formulas used for simulation and the parameters as defined by Pilon and Feldman (2006) are summarized in Table 3.1. The parameters μ (the reflex gain of the velocity feedback) and α (the slope of the exponential curve of muscle force generation) were adjusted to fit our experimental data.

For the simulation, we used a single-joint arm model with a total inertia of 0.09 kg*m^2/rad, which was about the average total inertia (hand, forearm and apparatus inertia) in our experiment. Perturbation was approximated by a rectangular torque pulse (amplitude=3, 3, 2 Nm, duration=100, 100, 80 ms for early, middle, late trigger) similar to that applied in the experiment. The control commands R and C were set to ramp signals which started to rise at movement initiation and reached final constant value 80 ms later. R started at 0 deg and terminated at 45 deg, C started at 5 deg and terminated at 25 deg. The proprioceptive delay (Δ) was set to 30 ms. All other model parameters shown in Fig. 3.2 and the corresponding equations are summarized in Table 3.1. The model was implemented and simulated in Matlab/Simulink.

Statistical analysis

Descriptive statistics were reported as mean and standard deviation in the text and in the table, and as mean and 95% confidence interval of the mean in the figures. All evaluated movement variables were compared between experimental data and model predictions using paired t tests. The squared coefficient of the correlation of joint position, velocity and torque between model and data was also used to evaluate the quality of the fit. For experimental data, the onset times of displacement, displacement speed and motor responses were compared with each other using paired t tests. Repeated measures ANOVA was performed to test the effect of trigger conditions on peak displacement, peak torque response, as well as the times of peak displacement and 60% compensation.

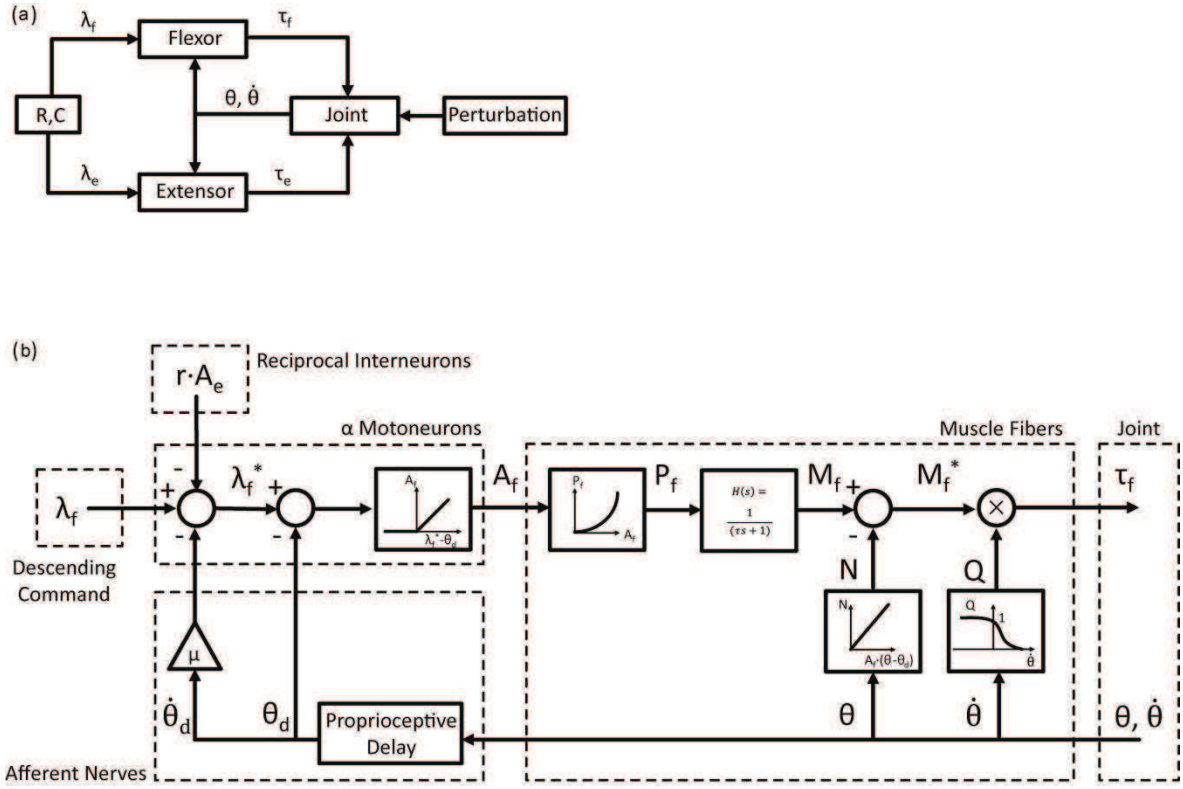

Figure 3.2: *Model of threshold position control of elbow joint (adopted from Pilon and Feldman 2006). Fig. 3.2a illustrates schematically how descending commands, flexor, extensor, and external perturbation interact in generating elbow joint motion. Fig. 3.2b demonstrates how the biceps (flexor) acts during force generation, mainly including α motoneurons and the muscle fibers that they innervate, as both shown in dashed blocks. The subscripts f, e, and d refer to flexor, extensor, and delay respectively. The whole process shown in (b) corresponds to the flexor block in (b). For clarity, the reciprocal interneuron is not shown in (a).*

Table 3.1 *(a) Relative equations for Fig. 2b. (b) Parameters for simulation in Fig. 3.2 and the equations in Table 3.1a. See definitions of variables and parameters in text.*

(a) Equations	(b) Parameters

$\lambda_f^* = \lambda_f - \mu \cdot \dot{\theta}_d - r \cdot A_e$
 	
$A_f = \begin{cases} \lambda_f^* - \theta_d, & \theta_d \le \lambda_f^* \\ 0, & \theta_d > \lambda_f^* \end{cases}$
 	
$P_f = a \cdot (e^{\alpha \cdot A_f} - 1)$
 	
$\theta_d = \theta(t - \Delta)$
 	
$N = k \cdot A_f \cdot (\theta - \theta_d)$
 	
$Q = \begin{cases} 0, & \dot{\theta} \ge v_m \\ \dfrac{1 - \frac{1}{v_m} \cdot \dot{\theta}_d}{1 + \frac{1}{b} \cdot \dot{\theta}_d}, & 0 \le \dot{\theta} < v_m \\ \dfrac{1 + \frac{1.3}{b'} \cdot \dot{\theta}_d}{1 + \frac{1}{b'} \cdot \dot{\theta}_d}, & \dot{\theta} < 0 \end{cases}$
	r=0.05;
	
	μ=0.06 s;
	
	a=1.2 Nm;
	
	α=0.045 deg^{-1};
	
	k=0.008 Nm*deg^{-2};
	
	v_m=700 deg/s;
	
	b=90 deg/s;
	
	$b' = -0.3 \cdot \frac{v_m \cdot b}{v_m + b} = -24$ deg/s;
	
	τ=10 ms;
	
	Δ=30 ms;

3.3 Results

Unperturbed Movements

Experimental results

The kinematics of unperturbed movements (trigger condition: middle) for one sample subject are shown as blue lines in Fig. 3.3a and b. The characteristic movement parameters, averaged across subjects are provided in Table 3.2. The movements showed a bell shape velocity and a biphasic torque profile. The peak burst of biceps EMG occurred during the acceleration phase of the fast movement, 23.9±18.4 ms before the first torque peak (blue lines in Fig. 3.3b and b). The first peak burst of the triceps occurred early in the deceleration phase of the fast movement, 84.6±70.2 ms before the second torque peak (blue lines in Fig. 3.3b and c).

Simulations

The model of Pilon and Feldman (2006) was first applied to predict kinematics, dynamics and EMG for unperturbed movements. The predicted patterns were similar to experimental data, as shown in Fig. 3f – j (blue lines). The kinematic and dynamic patterns matched the experimental patterns ($R^2 > 0.9$). For EMG the model predicted the main bursts of the biceps but for the triceps the predicted time course did not correlate strongly with the experimental data ($R^2 < 0.1$). This was due to the small signal amplitude in the triceps EMG (note the different scaling of Fig. 3.3d and e) which impaired the signal to noise ratio. Movement duration, peak velocity, peak torques and timing of first EMG peak bursts of simulated results for unperturbed movements did not differ significantly from the experimental data (T tests shown in Table 3.2).

To illustrate the model property in more detail the simulation results of Fig. 3.3f, g and i are reorganized in Fig. 3.4 and shown together with the descending command and the proprioceptive feedback of the flexor. Fig. 3.4 shows that the setting of the hypothetical control commands (dark blue line) precedes the movement onset. Particularly, the setting of monotonic and ramp-shaped control commands are already terminated at the peak initial flexor burst (green line), which is even before the peak velocity of the movement (St-Onge et al. 1997).

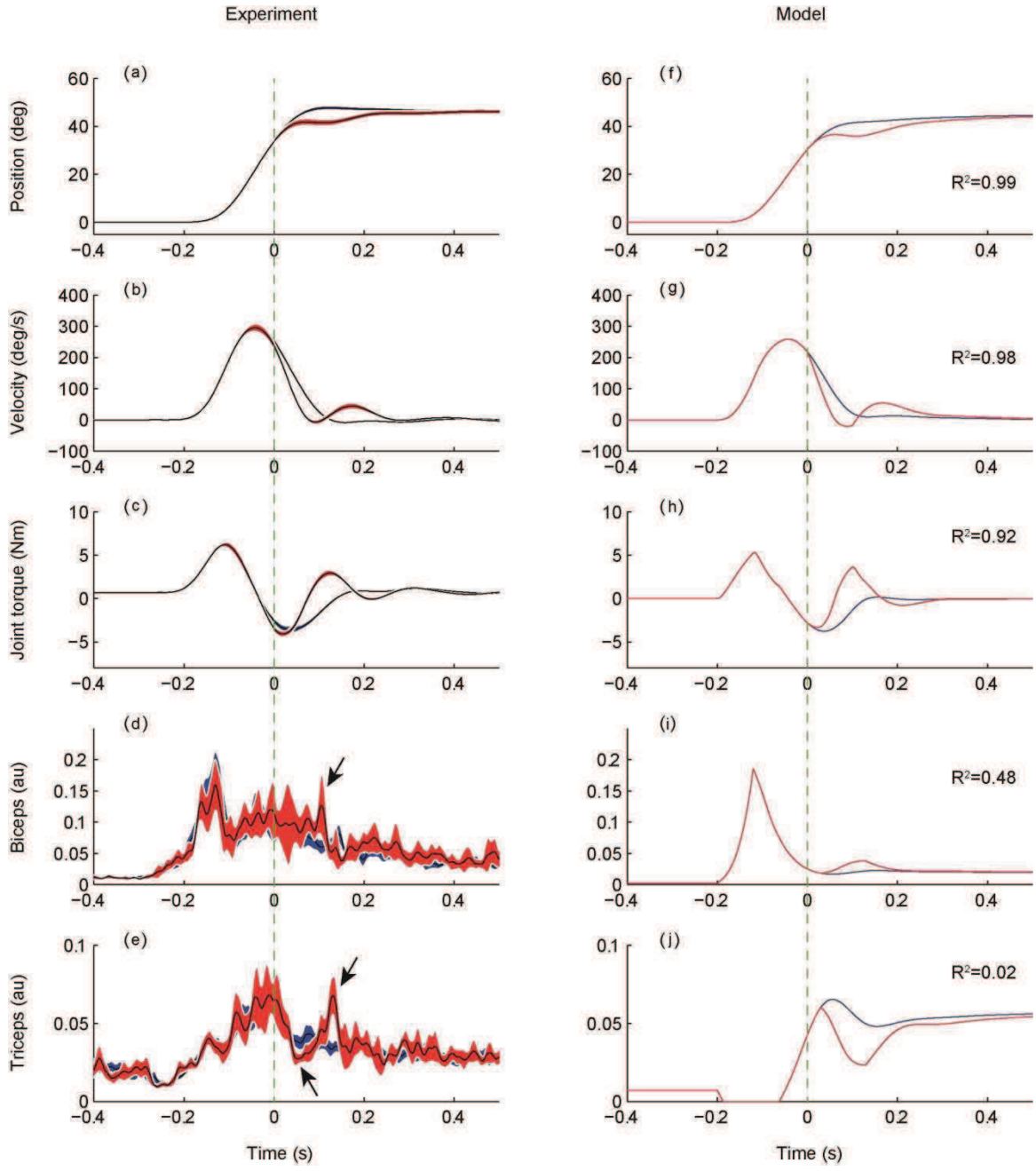

Figure 3.3: *Experimental results of one sample subject (a-e) with 95% confidence interval (shaded area) and model predictions (f-j) for the trigger condition middle (onset of perturbation shortly after peak velocity). Position, velocity, joint torque and EMG activities are shown for unperturbed (blue) and perturbed trials (red). Unit au shows normalized EMG activity. Time 0 is perturbation onset. The small arrows in d, e indicate the significant differences between perturbed and unperturbed EMG activities. For unperturbed movements the R square values between experimental data and model predictions are indicated.*

Table 3.2 *Experimentally observed movement characteristics of unperturbed movements (mean ± SD) and the corresponding predictions of the model. The times of peak velocity, 1st and 2nd peak torques and 1st biceps and triceps peak bursts are expressed with respect to movement start.*

	Experiment	Model	T test
Movement duration (ms)	296.0 ± 63.3	257.0	t(5)= 1.51, p= 0.192
Time of peak velocity (ms)	136.3 ± 36.9	117.0	t(5)= 1.28, p= 0.255
Time of 1st peak torque (ms)	54.9 ± 17.3	42.0	t(5)= 1.83, p= 0.127
Time of 2nd peak torque (ms)	217.6 ± 54.5	197.0	t(5)= 0.93, p= 0.397
Time of 1st biceps peak burst (ms)	31.0 ± 20.8	40.0	t(5)=-1.06, p= 0.337
Time of 1st triceps peak burst (ms)	133.0 ± 80.9	216.0	t(5)=-2.51, p= 0.054
Peak velocity (deg/s)	275.0 ± 62.0	258.6	t(5)= 0.65, p= 0.547
1st torque peak (Nm)	5.00 ± 1.58	5.30	t(5)=-0.48, p= 0.655
2nd torque peak (Nm)	-2.74 ±-1.38	-3.80	t(5)= 1.83, p= 0.127

Perturbation responses

Experimental results

The kinematics of perturbed movements for the middle trigger condition of one subject are shown as red lines in Fig. 3.3a and b. Joint angle was diverted by the perturbation and then converged back to the unperturbed one (Fig. 3.3a). The perturbed movement almost stopped and reaccelerated to reach the target (Fig. 3.3b). After perturbation onset (Time 0), the joint torque showed a second positive peak of 2.62±0.68 Nm at 134.3±17.0 ms (red line in Fig. 3.3c). The EMG activities showed much noisier patterns compared with torque patterns. However, a relatively short significant increase of the perturbed relative to the unperturbed biceps activity occurred shortly after perturbation onset (arrow in Fig. 3.3d). In the sample subject, triceps activity first decreased and then increased (arrows in Fig. 3.3e), but this pattern was not consistent across subjects.

The solid lines in Fig. 3.5 illustrate the perturbation effects and show displacement, displacement speed, torque response and biceps response. For the early, middle and late conditions, the peak displacement was -10.43±2.02, -6.99±1.45 and -3.84±1.72 deg, which corresponded to the decreasing perturbation torques. The end point deviation was 0.29±0.83, 0.17±0.87 and -0.01±0.66 deg respectively. Peak displacement decreased significantly for later trigger conditions (repeated measures ANOVA: $F_{(2,10)}$=106.49, $p<0.0001$). For the sample subject, as well as for all subjects, the main torque response had a positive sign (solid lines in Fig. 5G, H and I), which was opposite to the displacement (solid lines in Fig. 3.5a, b and c) and initial displacement speed (solid lines in Fig. 3.5d, e and f) for all three trigger conditions. The peak torque responses (early: 4.46±1.12, middle: 3.27±1.03, late: 1.85±0.65 Nm) decreased for later trigger conditions ($F_{(2,10)}$=48.70, $p<0.0001$). Perturbation always evoked a positive initial response in the biceps, as shown in Fig. 3.5j, k and l. The sign of initial EMG response in the triceps varied across subjects and perturbation conditions. For triceps EMG, 4, 3, and 2 out 6 subjects had a positive initial response in the early, middle and late trigger conditions respectively. Because of this inconsistency of the triceps response across subjects, the triceps response is not shown in Fig. 3.5.

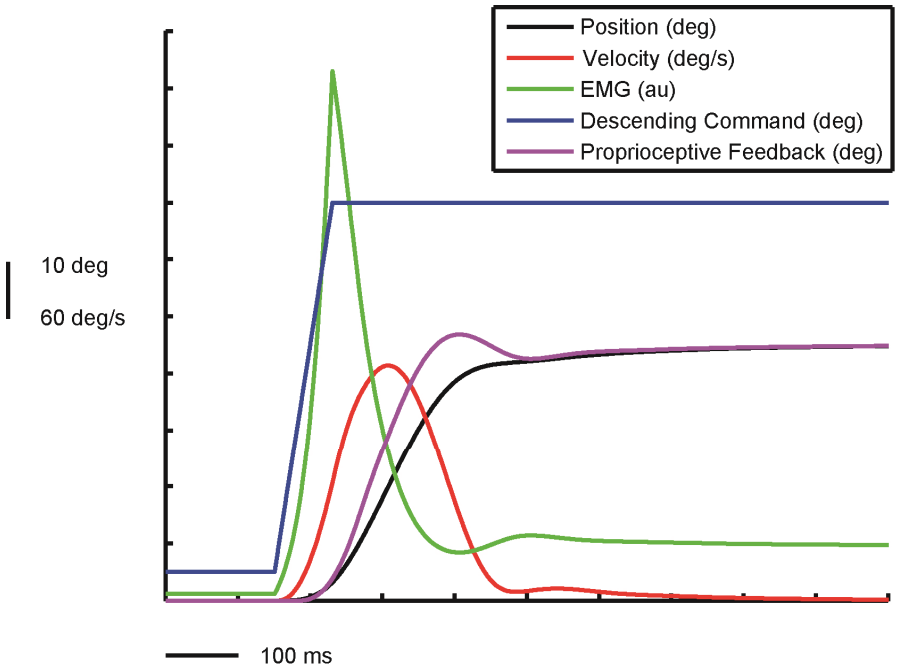

Figure 3.4: *Simulation of an unperturbed movement. The descending command, the proprioceptive feedback and the EMG of the flexor, as well as the joint position and velocity are shown. Note that joint position, descending command λf (=R+C) and proprioceptive feedback (including both length and velocity depended components, equal to the outputs of the block "Afferent Nerves" in Fig. 3.2) have the same unit deg. EMG is scaled and has arbitrary unit.*

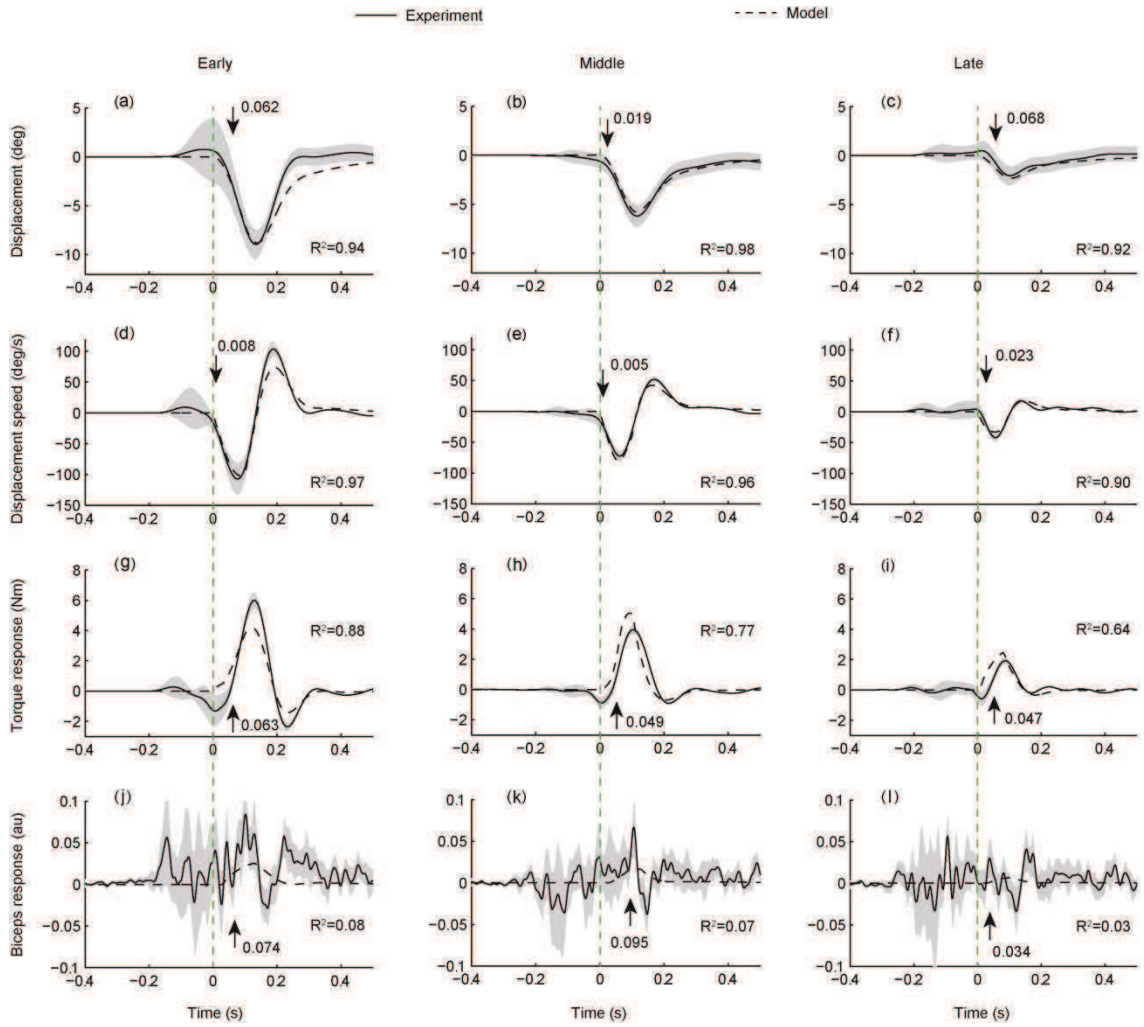

Figure 3.5: *Mean displacement, displacement speed, torque response and biceps response for all trigger conditions. Experimental results (solid lines, shaded area indicating the 95% confidence interval of the mean) and model prediction (dashed lines) are plotted together for the same subject as shown in Fig. 3.3. The results (second column) are equal to the corresponding differences between the red and blue lines from Fig. 3.3. The onset time of each variable (defined as the first time when the confidence interval of the mean does not include zero) is indicated by black arrows. Time 0 is the perturbation onset. The R square values between experimental data and model predictions are indicated.*

Simulations

The model of Pilon and Feldman (2006) was also applied to predict displacement, displacement speed, torque response and biceps response (dashed lines in Fig. 3.5a-l, which are equal to the difference between the red and blue lines in Fig. 3.3f-i). The patterns of displacement, displacement speed and torque response generally matched experimental results for all trigger conditions ($R^2 > 0.6$). The peak displacements predicted by the model (early: -8.79, middle: -5.81, late: -2.31 deg) did not significantly differ from the experimental group means (early: $t(5)=-1.99$, $p=0.104$, middle: $t(5)=-2.01$, $p=0.101$, late: $t(5)=-2.17$, $p=0.082$). The peak torque response of model prediction did not differ (t-test: $p>0.07$) from experimental data for early (predicted: 4.14 Nm) and late (predicted: 2.46 Nm) trigger conditions, but it did differ for the middle trigger condition (predicted: 5.05 Nm, $t(5)=-4.226$, $p<0.01$). After perturbation, an increase of biceps activity was predicted by the model (dashed lines in Fig. 3.5j and k). The details of these responses did not match the experimental results well ($R^2 < 0.1$). For most subjects (e.g. for the sample subject in Fig. 3.5j-k, solid lines), the biceps response had more than two peaks, while the model always predicted a single peak (Fig. 3.5j-k, dashed lines). However, these differences between model and data may be due to the large high frequency components of the inter-trial noise in the EMG and do not necessarily imply systematic differences between the actual and the modeled mean muscle activation.

Timing of perturbation response

The onset times of displacement, displacement speed, torque response and biceps responses with respect to perturbation onset are indicated as arrows for the sample subject in Fig. 3.5. The group data, also including triceps response onset, is summarized for all trigger conditions in Fig. 3.6. Averaged across all subjects and all perturbation conditions, the onset time (relative to perturbation onset) of the displacement was 54.2±6.6 ms, which was on average 41.1±3.2 ms later than that of the displacement speed (13.1±3.9 ms, paired t test: $t(5)=31.05$, $p<0.0001$), and did not differ from the onset time of the torque response (59.0±13.0 ms, paired t test: $t(5)=-0.646$, $p=0.547$). On average, the biceps response (latency: 66.8±19.6 ms) started 38.5±55.8 ms earlier (paired t test: $t(5)=-1.69$, $p=0.151$) than the triceps response (latency: 105.3±56.8 ms).

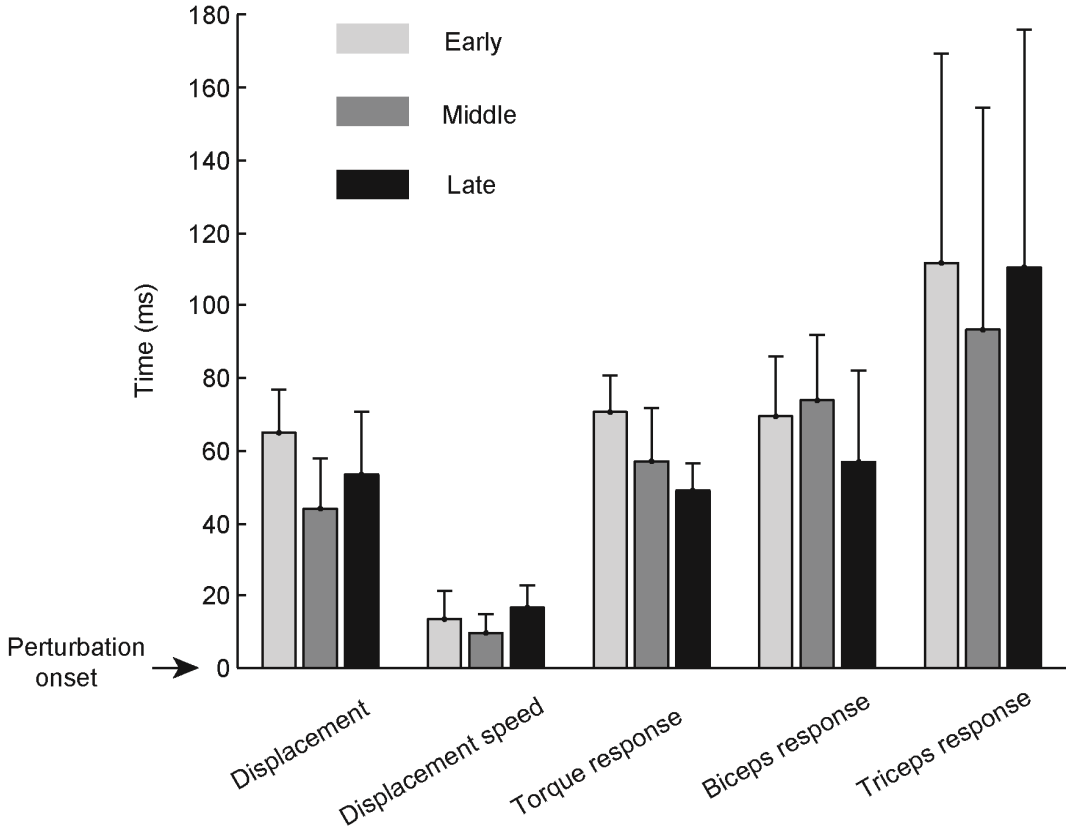

Figure 3.6: *Mean and 95% confidence interval of onset times of displacement, displacement speed, torque response and EMG responses of the biceps and triceps, across all subjects for three perturbation conditions (early, middle and late). Time 0 corresponds to perturbation onset.*

To quantify the efficiency of the perturbation response, the time of the displacement peak and the time of 60% compensation were computed, both with respect to perturbation onset. A comparison between experimental data and model predictions is shown in Fig. 3.7. For early, middle and late conditions, the displacement reached its peak 151.3±20.5 ms, 135.7±22.8 ms and 121.0±17.2 ms after perturbation onset, and the time of 60% compensation was 241.3±36.2, 230.5±33.0 and 232.5±42.6 ms. For all three trigger conditions, neither the time of peak displacement ($p>0.06$) nor that of 60% compensation ($p>0.54$) differed from those predicted by the model (see Fig. 3.7).

Next we analyzed whether the measured time of peak displacement and 60% compensation depended on trigger conditions. For the time of peak displacement, there was a main effect of trigger condition ($F_{(2,10)}$=78.15; p<0.001). Post hoc analysis revealed that the peak displacement in the early trigger condition occurred later than that in the late trigger condition (see Fig. 3.7). The time of 60% compensation did not depend significantly on trigger conditions ($F_{(2,10)}$=3.13; p=0.0879).

The role of intrinsic muscle properties in movement stabilization

To investigate the role of intrinsic muscle properties in generating motor responses to perturbation, we implemented four versions of the model that differed in the viscoelastic properties (Fig. 3.8). These different versions incorporated either (1, blue lines) no intrinsic viscoelastic properties of the muscles (in that case motor response to perturbation was only caused by the stretch reflex loop and interneuron inhibition), or (2, red lines) no intrinsic viscosity but intrinsic elasticity, or (3, green lines) no intrinsic elasticity but intrinsic viscosity, or (4, black lines) the full intrinsic properties as modeled by Pilon and Feldman (2006). When no intrinsic viscoelastic properties were present, the transient perturbation led to an atypical profile of the displacement with large oscillations (blue line in Fig. 3.8A). Adding the elastic component improved the performance of the system: it became more stable, although the compensation process was still delayed (red line in Fig. 3.8a). When viscosity was included, the system was able to compensate for the perturbation efficiently and it performed similarly well independent of whether the elastic component was present or not (black and green lines in Fig. 3.8a).

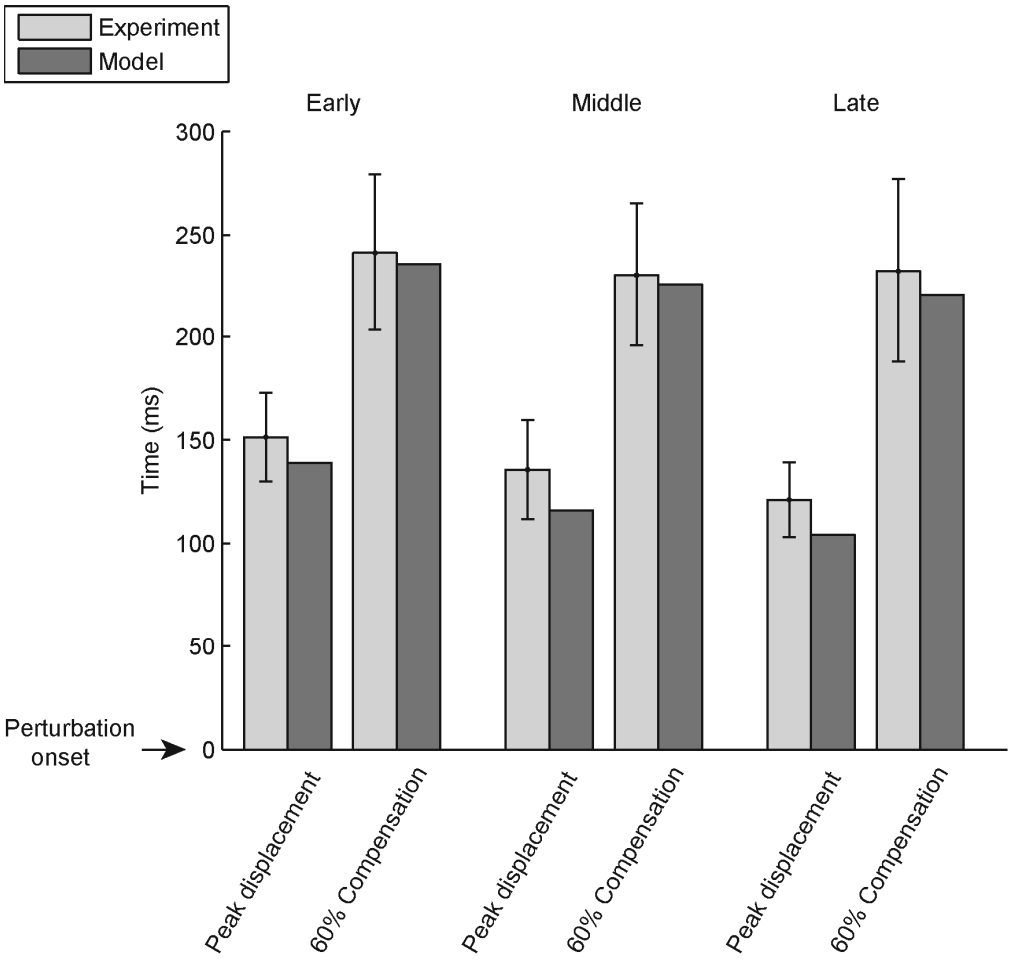

Figure 3.7: *Mean times of peak displacement and 60% compensation (i.e. time when the peak displacement decreased to 40% of its peak). For each trigger condition (early, middle and late), the experimental results and model simulation results are compared. Experimental results were from the data across all subjects. Error bars indicate the 95% confidence interval. Simulation is based on the same model (Pilon and Feldman 2006) as in Fig. 3.3f-j and Fig. 3.4 (dashed).*

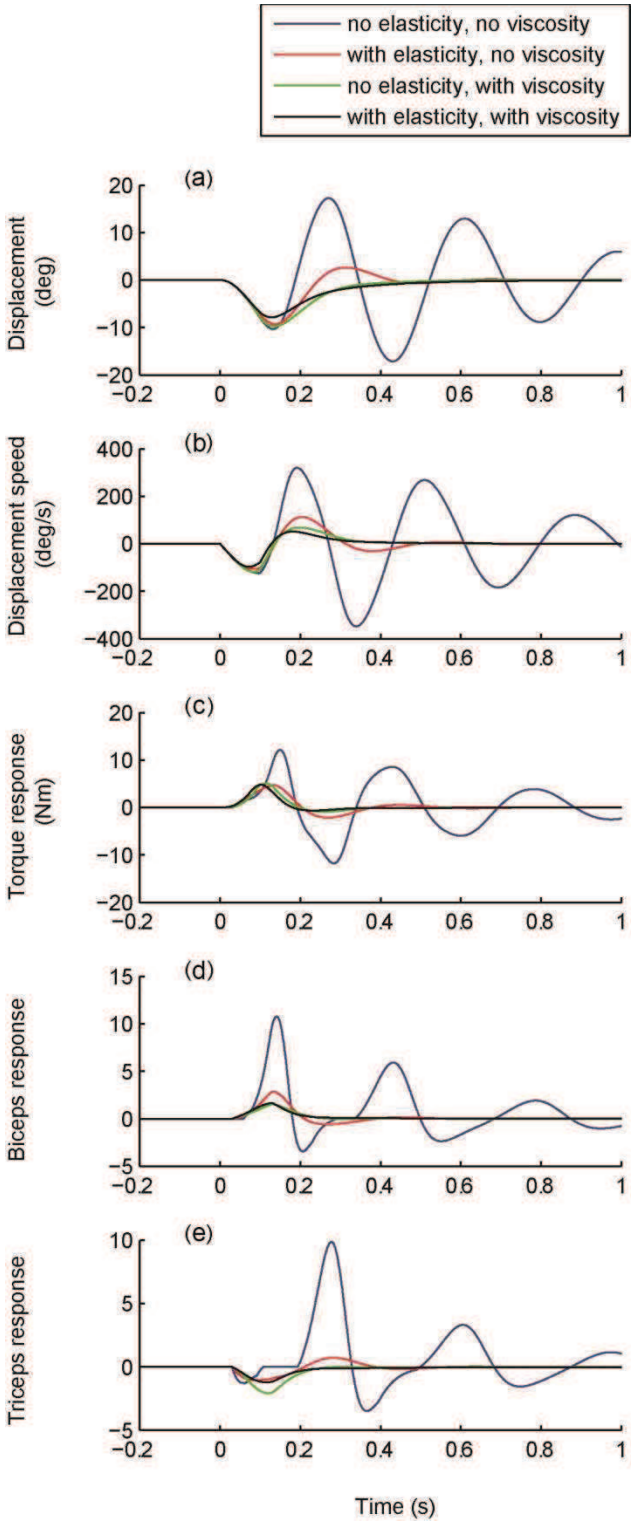

Figure 3.8: *Model prediction of displacement, displacement speed, torque response, biceps and triceps responses in the case of (1) no elasticity and no viscosity (2) with elasticity and no viscosity (3) no elasticity and with viscosity (4) with elasticity and with viscosity. The simulation results for the middle trigger condition were shown. Time zero is the perturbation onset.*

3.4 Discussion

In this study, we examined the motor responses to external perturbation during single-joint movement, and applied a physiologically plausible model accounting for many of the experimentally observed features. This model is based on the assumption that the central nervous system sets the α motoneuron threshold representing the input to a peripheral system which is characterized by the interaction between the spinal reflex loop, interneurons, muscle biomechanics and environment. Previous studies investigated movement generation with this model (St-Onge et al. 1997, Gribble et al. 1998, Pilon and Feldman 2006). In contrast, the current study focuses on the ability of the model to stabilize ongoing movements against small, unpredictable perturbations. The results show that the peripheral mechanisms implemented by this model explain the evoked motor responses induced by small perturbations at different movement phases. Furthermore, by manipulating the mechanical components of the model we demonstrated that changing intrinsic muscle properties while leaving the stretch reflex unchanged weakens stabilization and can even provoke instabilities.

Movement correction relying on peripheral feedback

Fig. 3.3a as well as Fig. 3.5a-c (solid lines) showed that, consistent with the results of Schmidt and McGown (1980) and Jaric et al. (1999), the arm reached the same final position regardless of the transient mechanical perturbation, suggesting that motor system was able to compensate for such a perturbation. The peak displacement after perturbation onset was reduced to 40% after about 230 ms after perturbation onset (Fig. 3.7). During this period the compensation for unexpected perturbation might involve different feedback-control mechanisms. However, it is unclear what kinds of feedback loops the motor system may have utilized for movement correction in our experiment.

The stretch reflex loop, together with intrinsic muscle properties, generates the most immediate responses to perturbations. As shown in Fig. 3.6, the onset times of both joint torque response and flexor EMG response were similar to the displacement onset, and were about 60 ms after perturbation onset. Other studies using stronger perturbations than the current study observed slightly smaller latencies of the EMG activity of about 50 ms (Pierrot-Deseilligny and Burke 2005, Crago et al. 1976). Induced by changes in muscle

length, the muscle opposes perturbations with minimal delay (<1 ms) due to the intrinsic viscoelastic property (Cecchi et al. 1986). This instantaneous reaction can contribute to the observed initial torque response.

In our experiments, the perturbation was sufficiently long (about 100ms) to possibly trigger also a long-latency response (Lewis et al. 2005). However, we were not able to disassociate such a supra-spinal response from a short-latency response (stretch reflex) based on the observed EMG responses. While the analysis of our experimental data alone does not exclude the presence of a long-latency response, our simulation results using the model proposed by Pilon and Feldman (2006) suggested that supra-spinal feedback control mechanisms were not essential to ensure the stability against transient small perturbations. Without a modification of central commands, the model implementing intrinsic muscle properties and stretch reflexes could explain the temporal kinematic and dynamic consequences for all three trigger conditions (Fig. 3.5a-i). During the first 230 ms after perturbation onset, the movement error was reduced by 60% (Fig. 3.7). The model was able to predict this compensation by only taking peripheral mechanisms into account in this time window. In addition, the model can explain peak displacement differences across trigger conditions by the differences in the perturbation amplitude. While the peak displacements decreased across trigger conditions due to decreased perturbation torques, the compensation process remained similarly efficient for all trigger conditions (Fig. 3.5a-c). This suggested that the feedback mechanisms are not necessarily state-dependent or time-variant.

Intentional corrections were highly unlikely to occur because (1) the perturbation was small enough to be sufficiently compensated (Sanes and Evarts 1983); (2) torque response became close to zero 200 ms after perturbation onset (Fig. 3.5g, h and i). Anticipatory compensation was impossible since all perturbed trials were randomly interspersed among unperturbed ones to reduce anticipation.

In summary, the model implementing only feedback of the stretch reflex loop and intrinsic muscle properties (see Fig. 3.2a) predicted the kinematic consequences and the motor responses, capturing most of their essential features (Fig. 3.5). The times of peak displacement and 60% compensation of the perturbation were well predicted for all trigger conditions (Fig. 3.7). It is not necessary to reconsider a modification of the control

commands due to a top-to-bottom influence of cortical control mechanisms on the stretch reflex loop and intrinsic muscle properties.

We emphasize the fundamental role of central control in ensuring the compensatory ability of peripheral mechanisms. In the applied model the stabilizing properties of the stretch reflex are essentially affected by the settings of the central commands. However, our simulation shows that small perturbations can be mostly compensated for without further online modification of central commands. This does not mean that central control mechanisms cannot achieve efficient compensation for suddenly occurring changes in arm dynamics (Bhushan and Shadmehr 1999) or for external perturbations including large perturbation amplitudes (Crevecoeur and Scott, 2014). Our simulation only suggests that under normal conditions and with small perturbations only, stretch reflex and intrinsic muscle properties cooperate efficiently. Adapting the reflex to changes in intrinsic muscle properties would probably take a long time and is beyond the scope of this study.

It is also important to note that, while in our experiments stretch reflex responses opposed transient small perturbations during single-joint reaching, this does not necessarily hold for other kinds of perturbations and multi-joint movements. For example with sinusoidal perturbations, due to the loop delay, the stretch reflex does not always resist the perturbation, and may even assist the perturbation (Bennett 1994, for a review see Hasan 2005). For multi-joint movements Soechting (1988) showed that the elbow stretch reflex in response to a brief force perturbation initially assisted the perturbation and later on the hand kinematics was restored near the end of the delayed movement. Thus, peripheral mechanisms alone do not seem to be sufficient to stabilize multi-joint movements, which is possibly due to the inherent complexity and instability of their dynamics (Zhang et al. 2014).

The role of intrinsic muscle properties in movement stabilization

Intrinsic muscle properties oppose perturbations by generating non-delayed length and velocity-dependent restoring forces. These intrinsic responses act before and are initially independent of the stretch reflex response. Another study (Kistemaker et al. 2007) investigated the responses of the arm to small transient perturbation during a movement using a more detailed muscle model (Hill 1938) than the one used in the current study.

Despite this simplification, both studies consistently conclude that perturbation responses can well be explained by the dynamic response of the peripheral musculoskeletal system without involving additional central control. This demonstrates the importance of low-level mechanisms for movement stabilization. In addition, we showed that changes in intrinsic muscle properties that were not accompanied by appropriate changes of the stretch reflex led to instability (blue lines in Fig. 3.8). This suggests that the stretch reflex and intrinsic muscle properties are well tuned to each other, since isolated changes of the viscosity predicted impaired stabilization. It seems that the intrinsic muscle properties cooperate in a synergistic way with the stretch reflex in order to efficiently compensate for transient small perturbations.

3.5 Conclusions

The present study showed that compensatory responses to transient perturbations during fast movements can be almost perfectly explained by peripheral mechanisms. Even though central control is essential for determining the response characteristics of the stretch reflex and intrinsic muscle properties, the response is a direct outcome of these peripheral mechanisms and does not necessarily involve an online modulation of central control signals.

Acknowledgements

We gratefully thank Katie Ogston for proof-reading the manuscript. This work was supported by the Research Training Group 1091 “Orientation and Motion in Space” of the Germany Research Foundation (DFG).

4. General Discussion

This thesis focused on the characteristics of rapid motor responses to transient perturbations during arm reaching movements. To minimize the perturbation-induced changes, the motor system generated compensatory responses, as observed in both studies of this thesis. The compensation process may involve motor responses from different levels of the motor system. Current studies indicate that peripheral motor system, which mainly includes stretch reflexes and intrinsic muscle properties, plays a major role in movement stabilization. The main findings of this thesis are summarized in the first section. The second section discusses the mechanisms of each component of the peripheral system in movement stabilization. The third section focuses on the limitation of peripheral system in movement stabilization. In certain cases, peripheral system failed to compensate the destabilizing perturbations. This is discussed in the framework of EPH theory in predicting perturbation responses during arm motion. In the fourth section, the implications for future directions are given.

4.1 Summary of main findings

The main findings of this thesis are: (1) key movement features such as bell-shaped hand velocity and biphasic joint torque are mostly preserved during unperturbed movements with full DoF arm; (2) motor system generates fast compensatory motor responses to external perturbations during full DoF reaching movements; (3) These responses do not necessarily reflect the modulation of central commands that directly react on the perturbation, and peripheral mechanisms can be sufficient at compensating for transient small perturbations; (4) the intrinsic muscle properties cooperate in a synergistic way with the stretch reflex at compensating for transient small perturbations.

Regarding the experimental part of the thesis, it provides an efficient experimental paradigm to measure perturbation responses during full DoF reaching movements, which have not been extensively studied before. Furthermore, this experimental setup was shown to be suitable for joint stiffness estimation during complex arm movements (Zhang et al. 2012).

Regarding the modelling and simulation parts of the thesis, the seven-DoF mechanical model of the arm was applied for quantifying joint torques. The single-joint arm model applied in the simulation study captures essential physiological features of arm reaching movements. It does not only predict fairly accurate kinematic and dynamic patterns of the movement, but is also able to generate reasonable EMG patterns.

Regarding the theoretical aspect of the thesis, the simulation of single-joint reaching movement validates the EPH in predicting motor responses to small perturbations. As such, this work is a strong support for EPH in handling single-joint movement.

4.2 Peripheral mechanisms in movement stabilization

(1) *Intrinsic muscle properties.* In the lowest level of the hierarchy, intrinsic muscle properties provide very useful and the most immediate responses to perturbations. The intrinsic muscle properties contribute to the initial torque responses, which start almost immediately with the perturbation-induced displacement onset (as shown in the experimental results of both studies). Without this mechanism, the system becomes unstable, even in the presence of small transient perturbations (as shown in simulation results with altered mechanical parameters in the second study). In some pathological conditions such as spasticity, changes in intrinsic muscle properties can be responsible for the increased muscle tone, i.e. hypertonia (Dietz et al. 1981). The role of intrinsic muscle properties in movement stabilization was also highlighted by the simulation study which implemented pure musculoskeletal model (Brown and Loeb 2000). This reflex-free model is able to react to applied perturbations, given certain preset patterns of muscle activations. For experimental tasks that require system stability, the intrinsic muscle properties can be also centrally modulated by changing the co-contraction of a muscle pair. For example, subjects can learn to interact with uncertain environments by increasing the co-contraction, leading to an increase of joint stiffness in the direction of instability (Franklin et al. 2003). Although this is an inefficient way of using energy, the motor system is able to achieve stability. As such, the intrinsic muscle properties are also termed as “pre-reflexes” (Brown and Lob 2000). Thus, the intrinsic muscle properties have the instantaneous reaction to perturbation and contribute to system stability.

(2) *Golgi tendon reflexes.* The Golgi tendon reflex causes muscle relaxation and protects the tendon from damage when tendon tension becomes too high. As part of the low-level control, it may also affect the musculoskeletal system dynamics (Alexander 2002, Kistemarker et al. 2013). The Golgi tendon reflex is generally considered to be less important in motor control, partly because it is less sensitive than stretch reflex and its function is less clear. Recently, some modelling studies have considered this mechanism (Mileusnic and Loeb 2006, Kistemarker et al. 2013). In current thesis this tendon feedback was neglected due to the complexity of the modelling. For future modelling studies, such a mechanism can be included to have a more complete description of the bottom-level motor system.

(3) *Stretch reflexes.* The contribution of stretch reflex to system stability can depend on perturbation and movement types. In reaction to small transient perturbations, the stretch reflex generates compensatory motor response (as shown by experimental results of the second study). In this case, it contributes to movement stabilization. However, if the muscle is continuously stretched, the stretch reflex becomes weaker (Nichols and Houk 1976), suggesting that stretch reflex may not be sufficient to oppose long-lasting perturbations. Besides, due to the loop delay, the stretch reflexes may even assist perturbations (Hasan 2005). When encountering oscillation perturbation with high frequency, the evoked EMG responses can have a phase lag with respect to perturbation (Bennett 1994) and thus contribute to instability of the system. For multi-joint movements Soechting (1988) showed that the elbow stretch reflex in response to a brief force perturbation initially assisted the perturbation and later on the hand kinematics was restored near the end of the delayed movement.

In short summary: (1) the peripheral mechanisms generate rapid responses to external perturbations. (2) In certain cases of transient small perturbations (as in the two studies of this thesis), they cope efficiently with perturbations, while for other types of perturbations or movements, the peripheral mechanisms alone may not be sufficient to ensure system stability. This leads to the next section of the discussion about the limitation of peripheral systems at compensating for perturbations.

4.3 Influence of central control on peripheral mechanisms

As demonstrated before, peripheral mechanisms are efficient at compensating for small transient perturbations. This compensation thus ensures movement stability without a change of high-level control commands. However, some studies showed that the motor system failed to compensate movement errors in the case of certain destabilizing perturbations, such as Coriolis force field (Lackner and DiZio 1994, Dizio and Lackner 1995). In those cases, the top-level control command could be modified during the movement (Feldman and Latash 2005) although subjects did not intentionally react to perturbations. This unintentional change of control commands can lead to a movement error in the final state.

A recent study (Zhou et al. 2014), in which the author of this thesis contributed as a co-author[1], explored this unintentional change in more details about its spatial and temporal characteristics, in a different experimental scenario. The task was firstly to hold a robot handle at an initial position against a base-line force produced by the robot. The subject was instructed not to interfere voluntarily with the effects of the upcoming perturbation. That means, the subject should neither resist to the perturbation nor relax the arm intentionally. A smooth increase of the robot force elicited arm motion away from the initial position. The robot force was kept constant for a certain dwell time and then it dropped to the base-line level. As a consequence, the hand moved towards the initial position and stopped short of the initial position. To probe this characteristic quantitatively, the perturbation amplitude and its duration (i.e. dwell time) were manipulated (4 magnitudes and 9 dwell times). The results showed that an increase of the dwell time (up to about 8 seconds) led to larger final undershoot. The final undershoot also increased with larger perturbation magnitude. From the perspective of EPH, these results suggested that the final undershoot was due to an unintentional change of the control command, which depended on the perturbation characteristics.

In this case, arm motion was not stabilized (large deviation during dwell time) and movement error was not corrected (final undershoot). It is possible that strong and long-lasting perturbations could have significant effect on the central control and cause an

[1] This study was performed at the motor control lab of Prof. M Latash at Pennsylvania State University during a research stage of one month, when the author helped perform the experiment. After the research stage, the author helped analyze the data and write part of the manuscript.

unintentional change of control command, even though subjects did not voluntarily alter the control command (i.e. not voluntarily intervene). Subsequently this unintentional change of control command modified the parameters of peripheral mechanisms such as the threshold muscle length. As a consequence, the arm did not reach the same final position. According to EPH, the peripheral system can only function under central control (by centrally setting the threshold muscle length). Thus, the peripheral system depends highly on central control commands. In the study of Zhou et al. (2014), both R and C commands could have been altered by the effect of the long-lasting perturbations.

In a nutshell, the compensatory ability of the peripheral mechanisms is determined by central control. Perturbation characteristics can cause unintentional change of central control commands, which consequently affects the ability of peripheral mechanisms in movement stabilization.

4.4 Implications for future research

First of all, it is worthwhile to highlight the methodological contribution of the first study. Unconstrained movements (i.e. with full DoFs of the arm) are very common in daily life and are inherently unstable due to the complex dynamics. While most of experimental studies induced certain constraints of movement dimensions (e.g. on planar surface), the current methodology provides both useful experimental and analytical tools for studying unconstrained arm movements in three dimensional space.

Second, the physiological model in the second study should be elaborated to explain the failures of the motor system to prevent movement errors in the presence of certain destabilizing perturbations (Lackner and Dizio 1994, Popescu and Rymer 2000, Hinder and Milner 2003, Zhou et al. 2014), which have been mentioned in section 4.3. The current physiological model uses central control signals that settle early during the movement, whereas a more elaborated model may incorporate a transcortical feedback loop, which takes the peripheral feedbacks into account for modifying control commands.

Besides, the current physiological model should implement more details of intrinsic muscle properties and reflexes, such as Hill-type series elasticity as well as Golgi tendon reflexes (Kistemarker et al. 2007, 2013). Especially, due to the presence of series elasticity (Hill

1938), muscle spindle firing is related to muscle fiber length, which is not exactly related to joint angle while in this thesis the stretch reflex was modelled as feedback on joint angle and joint angular velocity. Considering the stability properties of the system, this series elastic component can be also essential for simulations of isometric torque production (Pilon and Feldman 2006).

Finally, this thesis opens a future direction for clinical studies. The experimental paradigm of single-joint reaching in the second study does not demand too much effort or movement complexity, and thus can be suitable to test patients with motor disorders, such as spasticity, dystonia, ataxia and Parkinson's disease. Furthermore, the simulation study in the framework of EPH underlies essential physiological features of motor control and can be used to analyze these disordered movements. Similar applications in clinical studies are as yet few. For example, experimental measurement of threshold joint angles showed that spastic hemiparetic patients have smaller stretch reflex thresholds compared to normal subjects (Levin and Feldman 1994, Jobin and Levin 2000). This decrease might be either due to disordered top-bottom regulation or changes of bottom-level peripheral properties. To distinguish different sources of the abnormal threshold values, a reconstruction of central commands by simulation can be useful. Therefore both experimentally and theoretically, the current scheme can be applicable and meaningful to study a variety of motor diseases.

Bibliography

Adamovich SV, Levin MF, Feldman AG (1997) Central modifications of reflex parameters may underlie the fastest arm movements. J Neurophysiol 77: 1460-1469

Alexander RM (2002) Tendon elasticity and muscle function. Comp Biochem Physiol A Mol Integr Physiol 133(4): 1001-1011

Atkeson CG, Hollerbach JM (1985) Kinematic features of unrestrained vertical arm movements. J Neurosci 5(9): 2318-2330

Bennett DJ, Hollerbach JM, Xu Y, Hunter IW (1992) Time-varying stiffness of human elbow joint during cyclic voluntary movement. Exp Brain Res 88 (2):433-442

Bennett DJ (1993) Electromyographic responses to constant position errors imposed during voluntary elbow joint movement in human. Exp Brain Res 95: 499-508

Bennett DJ (1994) Stretch reflex responses in the human elbow joint during a voluntary movement. J Physiol 474(2): 339-351

Bernstein NA (1967) The co-ordination and regulation of movements. Pergamon Press

Berret B, Bonnetblanc F, Papaxanthis C, Pozzo T (2009) Modular Control of Pointing beyond Arm's Length. J Neurosci 29 (1):191-205

Bhushan, N, Shadmehr, R (1999) Computational nature of human adaptive control during learning of reaching movements in force fields. Biol Cybern 81 (1), 39-60

Biess A, Liebermann DG, Flash T (2007) A computational model for redundant human three-dimensional pointing movements: Integration of independent spatial and temporal motor plans simplifies movement dynamics. J Neurosci 27(48): 13045-13064

Brown SH, Cooke JD (1981) Responses to force perturbations preceding voluntary human arm movements. Brain Res 220: 350-355

Brown I, Loeb G (2000) A reductionist approach to creating and using neuromusculoskeletal models. In: Winters J, Crago P (eds) Biomechanics and neural control of posture and movement. Springer New York, pp 148-163

Burdet E, Osu R, Franklin DW, Yoshioka T, Milner TE, Kawato M (2000) A method for measuring endpoint stiffness during multi-joint arm movements. J Biomech 33(12): 1705-1709

Burdet E, Tee KP, Mareels I, Milner TE, Chew CM, Franklin DW, Osu R, Kawato M (2006) Stability and motor adaptation in human arm movements. Biol Cybern 94(1): 20-32

Cecchi G, Griffiths PJ, Taylor S (1986) Stiffness and force in activated frog skeletal muscle fibers. Biophys J 49(2): 437-451

Crevecoeur F, Scott SH (2014) Beyond muscles stiffness: importance of state-estimation to account for very fast motor corrections. PLoS Comput Biol 10 (10):e1003869

Crago PE, Houk JC, Hasan Z (1976) Regulatory actions of human stretch reflex. J Neurophysiol 39(5): 925-935

Darainy M, Towhidkhah F, Ostry D (2007) Control of hand impedance under static conditions and during reaching movement. J Neurophysiol 97(4): 2676-268

d'Avella A, Portone A, Fernandez L, Lacquaniti F (2006) Control of fast-reaching movements by muscle synergy combinations. J Neurosci 26 (30):7791-7810

Dietz V, Quintern J, Berger W (1981) Electrophysiological studies of gait in spasticity and rigidity. Evidence that altered mechanical properties of muscle contribute to hypertonia. Brain 104(3): 431-449

Dietz V, Quintern J, Berger W (1985) Afferent control of human stance and gait: evidence for blocking of group I afferents during gait. Exp Brain Res 61(1):153-163

Dizio P, Lackner JR (1995) Motor adaptation to Coriolis force perturbations of reaching movements: endpoint but not trajectory adaptation transfers to the nonexposed arm. J Neurophysiol 74:1787–1792

Fan J, He JP, Tillery SIH (2006) Control of hand orientation and arm movement during reach and grasp. Exp Brain Res 171 (3):283-296

Feldman AG (1966) Functional tuning of the nervous system with control of movement or maintenance of a steady posture. II. Controllable parameters of the muscle. Biophysics 11: 565–578

Feldman AG, Orlovsky GN (1972) The influence of different descending systems on the tonic stretch reflex in the cat. Exp Neurol 37 (3):481-494

Feldman AG (1986) Once more on the equilibrium-point hypothesis (λ model) for motor control. J Motor Behav 18: 17–54

Feldman AG (2011) Space and time in the context of equilibrium-point theory. WIREs Cogn Sci, 2: 287-304

Feldman AG, Latash ML (2005) Testing hypotheses and the advancement of science: recent attempts to falsify the equilibrium point hypothesis. Exp Brain Res 161 (1): 91-103

Feldman AG, Levin MF (1995) The origin and use of positional frames of reference in motor control. Behav Brain Sci 18: 723-744

Flash T, Hogan N (1985) The coordination of arm movements – an experimentally confirmed mathematical model. J Neurosci 5(7): 1688-1703

Franklin DW, Osu R, Burdet E, Kawato M, Milner TE (2003) Adaptation to stable and unstable dynamics achieved by combined impedance control and inverse dynamics model. J Neurophysiol 90: 3270–3282

Frolov AA, Prokopenko RA, Dufosse M, Ouezdou FB (2006) Adjustment of the human arm viscoelastic properties to the direction of reaching. Biol Cybern 94(2): 97-10

Fung YC (1993) Biomechanics: Mechanical Properties of Living Tissues. Springer New York

Gomi H, Kawato M (1997) Human arm stiffness and equilibrium-point trajectory during multi-joint movement. Biol Cybern 76(3): 163-171

Gottlieb GL, Song QL, Almeida GL, Hong DA, Corcos D (1997) Directional control of planar human arm movement. J Neurophysiol 78(6): 2985-2998

Gribble PL, Ostry DJ, Sanguineti V, Laboissiere R (1998) Are complex control signals required for human arm movement? J Neurophysiol 79: 1409-1424

Grimme B, Lipinski J, Schöner G (2012) Naturalistic arm movements during obstacle avoidance in 3D and the identification of movement primitives. Exp Brain Res 222(3):185-200

Grinyagin IV, Biryukova EV, Maier MA (2005) Kinematic and dynamic synergies of human precision-grip movements. J Neurophysiol 94(4): 2284-2294

Hasan Z (2005) The human motor control system's response to mechanical perturbation: Should it, can it, and does it ensure stability? J Motor Behav 37(6): 484-493

Hays AV, Richmond BJ, Optican LM (1982) Unix-based multiple process system for realtime data acquisition and control. WESCON Proc Conf 2: 100-105

Hill AV (1938) The heat of shortening and the dynamic constants of muscle. Proc R Soc Lond Ser B 126: 136-195

Hinder MR, Milner TE (2003) The case for an internal dynamics model versus equilibrium point control in human movement. J Physiol 549: 953–963

Hogan N (1985) The mechanics of multi-joint posture and movement control. Biol Cybern 52(5): 315-331

Jaric S, Milanovic S, Blesic S, Latash ML (1999) Changes in movement kinematics during single-joint movements against expectedly and unexpectedly changed inertial loads. Hum Mov Sci 18(1): 49-66

Jindrich D, Courtine G, Liu J, McKay H, Moseanko R, Bernot T, Roy R, Zhong H, Tuszynski M, Reggie Edgerton V (2011) Unconstrained three-dimensional reaching in Rhesus monkeys. Exp Brain Res 209(1): 35-50

Jobin A, Levin MF (2000) Regulation of stretch reflex threshold in elbow flexors in children with cerebral palsy: a new measure of spasticity. Dev Med Child Neurol 42: 531–540

Kawato M (1999) Internal models for motor control and trajectory planning. Curr Opini Neurobiol 9(6): 718–727

Khatib O (1987) A unified approach for motion and force control of robot manipulators – the operational space formulation. IEEE J Robot Autom 3(1): 43-53

Kimura T, Haggard P, Gomi H (2006) Transcranial magnetic stimulation over sensorimotor cortex disrupts anticipatory reflex gain modulation for skilled action. J Neurosci 26 (36): 9272-9281

Kistemaker DA, Van Soest AK, Bobbert MF (2007) Equilibrium point control cannot be refuted by experimental reconstruction of equilibrium point trajectories. J Neurophysiol 98(3): 1075-1082

Kistemaker DA, Van Soest AJ, Wong JD, Kurtzer I, Gribble PL (2013) Control of position and movement is simplified by combined muscle spindle and Golgi tendon organ feedback. J Neurophysiol 109(4): 1126-1139

Krueger M, Eggert T, Straube A (2011) Joint angle variability in the time course of reaching movements. Clin Neurophysiol 122(4): 759-766

Krueger M, Borbely B, Eggert T, Straube A (2012) Synergistic control of joint angle variability: Influence of target shape. Hum Mov Sci 31(5): 1071-1089

Krylow AM, Rymer WZ (1997) Role of intrinsic muscle properties in producing smooth movements. IEEE Trans Biomed Eng 44(2): 165-176

Kurtzer IL, Pruszynski JA, Scott SH (2008) Long-latency reflexes of the human arm reflect an internal model of limb dynamics. Curr Biol 18(6): 449-453

Lackner JR, DiZio P (1994) Rapid adaptation to Coriolis force perturbations of arm trajectory. J Neurophysiol 72:1–15

Lacquaniti F, Soechting JF (1982) Coordination of arm and wrist motion during a reaching task. J Neurosci 2(4): 399-408

Lacquaniti F, Soechting JF (1984) Behavior of the stretch reflex in a multi-jointed limb. Brain Res 311(1): 161-166

Lacquaniti F, Soechting JF (1986a) EMG Responses to load perturbations of the upper limb – effect of dynamic coupling between shoulder and elbow motion. Exp Brain Res 61(3): 482-496

Lacquaniti F, Soechting JF (1986b) Responses of mono- and bi-articular muscles to load perturbations of the human arm. Exp Brain Res 65(1): 135-144

Lacquaniti F, Soechting JF, Terzuolo SA (1986) Path constraints on point-to-point arm movements in three-dimensional space. Neuroscience 17(2): 313-324

Latash ML (1994) Control of fast elbow movement: a study of electromyographic patterns during movements against unexpectedly decreased inertial load. Exp Brain Res 98: 145-152

Lee DP, Corcos DM, Shemmell J, Leurgans S, Hasan Z (2008) Resolving kinematic redundancy in target-reaching movements with and without external constraint. Experimental Brain Res 191(1): 67-81

Lee RG, Tatton WG (1982) Long latency reflexes to imposed displacements of the human wrist: dependence on duration of movement. Exp Brain Res 45: 207-216

Levin MF, Feldman AG (1994) The role of stretch reflex threshold regulation in normal and impaired motor control. Brain Res 657: 23–30

Lewis GN, Perreault EJ, MacKinnon CD (2005) The influence of perturbation duration and velocity on the long-latency response to stretch in the biceps muscle. Exp Brain Res 163: 361-369

Mah CD (2001) Spatial and temporal modulation of joint stiffness during multijoint movement. Exp Brain Res 136(4): 492-506

Matthews PBC (1959) The dependence of tension upon extension in the stretch reflex of the soleus muscle of the decerebrate cat. J Physiol 147(3): 521–546.

Mattos DJS, Latash ML, Park E, Kuhl J, Scholz JP (2011) Unpredictable elbow joint perturbation during reaching results in multijoint motor equivalence. J Neurophysiol 106(3): 1424-1436

Mileusnic MP, Loeb GE (2006) Mathematical models of proprioceptors. II. Structure and function of the Golgi tendon organ. J Neurophysiol 96: 1789-1802

Milner TE (1993) Dependence of elbow viscoelastic behavior on speed and loading in voluntary movements. Exp Brain Res 93: 177-180

Morasso P (1981) Spatial control of arm movemenmts. Exp Brain Res 42(2): 223-227

Niu CM, Corcos DM, Shapiro MB (2012) Suppression of proprioceptive feedback control in movement sequences through intermediate targets. Exp Brain Res 216: 191-201

Niu CM, Corcos DM, Shapiro MB (2010) Temporal shift from velocity to position proprioceptive feedback control during reaching movements. J Neurophysiol 104: 2512-2522

Norman RW, Komi PV (1979) Electromechanical delay in skeletal muscle under normal movement conditions. Acta Physiol Scand 106 (3): 241-248

Ostry DJ, Feldman AG (2003) A critical evaluation of the force control hypothesis in motor control. Exp Brain Res 153(3): 275-288

Pierrot-Deseilligny E, Burke D (2005) The circuitry of the human spinal cord: its role in motor control and movement disorders. Cambridge University Press

Pilon JF, Feldman AG (2006) Threshold control of motor actions prevents destabilizing effects of proprioceptive delays. Exp Brain Res 174: 229-239

Popescu FC, Hidler JM, Rymer WZ (2003) Elbow impedance during goal-directed movements. Exp Brain Res 152(1): 17-28

Popescu FC, Rymer WZ (2000) End points of planar reaching movements are disrupted by small force pulses: an evaluation of the hypothesis of equifinality. J Neurophysiol 84: 2670–2679

Pozzo T, Stapley PJ, Papaxanthis C (2002) Coordination between equilibrium and hand trajectories during whole body pointing movements. Exp Brain Res 144(3): 343-350

Rothwell JC, Traub MM, Marsden CD (1982) Automatic and “voluntary” responses compensating for disturbances of human thumb movements. Brain Res 248(1): 33-41

Sainburg RL, Ghilardi MF, Poizner H, Ghez C (1995) Control of limb dynamics in normal subjects and patients without proprioception. J Neurophysiol 73(2): 820-835

Sanes JN, Evarts EV (1983) Effects of perturbations on accuracy of arm movements. J Neurosci 3(5): 977-986

Schmidt RA (1975) A schema theory of discrete motor skill learning. Psychol Rev 82(4): 225-260

Schmidt RA, McGown C (1980) Terminal accuracy of unexpectedly loaded rapid movements: evidence for a mass-spring mechanism in programming. J Motor Behav 12: 149-161

Schütz C, Schack T (2013) Motor primitives of pointing movements in a three-dimensional workspace. Exp Brain Res 227(3): 355-365

Scott SH (2012) The computational and neural basis of voluntary motor control and planning. Trends Cogn Sci 16(11): 541-549

Shadmehr R, Krakauer JW (2008) A computational neuroanatomy for motor control. Exp Brain Res 185: 359-381

Shapiro MB, Gottlieb GL, Corcos DM (2004) EMG responses to an unexpected load in fast movements are delayed with an increase in the expected movement time. J Neurophysiol 91: 2135-2147

Sherrington CS (1906) The integrative action of the nervous system. Scribner

Smeets JBJ, Erkelens CJ, Denier van der Gon JJ (1990) Adjustments of fast goal-directed movements in response to an unexpected inertial load. Exp Brain Res 81: 303-312

Smeets JBJ, Erkelens CJ, Denier van der Gon JJ (1995) Perturbations of fast goal-directed arm movements: different behaviour of early and late EMG-responses. J Motor Behav 27: 77-88

Soechting JF (1988) Effect of load perturbations on EMG activity and trajectories of pointing movements. Brain Research 451(1-2): 390-396

Soechting JF, Lacquaniti F (1988) Quantitative evaluation of the electromyographic responses to multidirectional load perturbations of the human arm. J Neurophysiol 59 (4): 1296-1313

Soechting JF, Lacquaniti F (1989) An assessment of the existence of muscle synergies during load perturbations and intentional movements of the human arm. Exp Brain Res 74(3): 535-548

St-Onge N, Adamovich SV, Feldman AG (1997) Control processes underlying elbow flexion movements may be independent of kinematic and electromyographic patterns: experimental study and modelling. Neuroscience 79: 295-316

Thomas JS, Corcos DM, Hasan Z (2005) Kinematic and kinetic constraints on arm, trunk, and leg segments in target-reaching movements. J Neurophysiol 93(1): 352-364

Todorov E (2005) Stochastic optimal control and estimation methods adapted to the noise characteristics of the sensorimotor system. Neural Comput 17(5): 1084-1108

Todorov E, Li W, Pan X (2005) From task parameters to motor synergies: A hierarchical framework for approximately-optimal control of redundant manipulators. J Robotic Syst 22(11): 691–710

Tolambiya A, Thomas E, Chiovetto E, Berret B, Pozzo T (2011) An ensemble analysis of electromyographic activity during whole body pointing with the use of support vector machines. PLoS One 6(7): e20732

Van der Helm FC, Schouten AC, de Vlugt E, Brouwn GG (2002) Identification of intrinsic and reflexive components of human arm dynamics during postural control. J Neurosci Meth 119(1): 1-14

Von Holst E, Mittelstaedt H (1950) Das Reafferezprinzip. Wechselwirkungen zwischen Zentralnerven-system und Peripherie, Naturwiss 37:467–476

Wei KL, Wert D, Kording K (2010) The nervous system uses nonspecific motor learning in response to random perturbations of varying nature. J Neurophysiol 104(6): 3053-3063

Winter DA (2009) Biomechanics and motor control of human movement. Hoboken, N.J., Wiley

Wolpert DM, Miall RC, Kawato M (1998) Internal models in the cerebellum. Trends Cogn Sci 2 (9): 338-347

Won J, Hogan N (1995) Stability properties of human reaching movements. Exp Brain Res 107(1): 125-136

Zhang L, Straube A, Eggert T (2014) Torque response to external perturbation during unconstrained goal-directed arm movements. Exp Brain Res 232(4): 1173-1184

Zhang L, Straube A, Eggert T (Submitted) Peripheral mechanisms compensate efficiently for small perturbations of arm movements.

Zhang L, Eggert T, Glasauer S, Straube A (2012) Stiffness estimation during complex arm movements. Society for Neuroscience. Abstract.

Zhou T, Zhang L, Latash M (2014) Characteristics of unintentional movements by a multi-joint effector. J Motor Behav. In press.

Acknowledgements

I would like to express my sincere gratefulness to everyone that has guided me, encouraged me, supported me, helped me, and motivated me through my doctoral study and life.

My deepest gratitude goes first to Prof. Andreas Straube, my principle supervisor and my doctoral “grandfather”. I thank him for offering me the opportunity to carry out my doctoral projects in his group. He gave me lots of freedom to conduct the research and supported me strongly all the time. It was great to have him always being there. He is also a nice trip advisor that made me enjoy the Bavarian life as native.

I would like to express my sincere gratitude to Dr. Thomas Eggert, my second supervisor and my doctoral “father”. I thank him gratefully for his kind guidance as well as critical instructions, which contribute largely to my doctoral research. He taught me how to think and write logically as a scientist. This would be invaluable for me to make future progress in scientific career. Besides science, he is a great guide who led me to the brilliant world of the European art.

I gratefully thank Prof. Joachim Hermsdöfer (TUM) to be a member of my thesis committee. He has provided me with useful feedbacks and objective evaluations on my research work.

I would like to thank Researching Training Group 1091. It supported me in all aspects of my doctoral research, and offered me extraordinary opportunities to interact with other people in science. Special sincere thanks go to Maj-Catherine Botheroyd, who has been always kind and helpful to support me.

I want to thank Prof. Mark Latash (PennState) and Prof. Anatol Feldman (UMontreal). I really enjoyed the cooperation with Prof. Latash’s group and had an amazing time with his people there in State College. I thank Prof. Feldman for his patience in teaching me to comprehend his idea of motor control theory. We had several wonderful discussions during summer schools and his wisdom inspired me a lot in motor control research.

I owe heartily gratitude to Prof. Elmar Schrüfer (TUM). He has been taking good care of me (as well as many other Chinese students) ever since my first trip to Germany. His courtesy and enthusiasm have set a good example for me to follow.

Many thanks would go to colleges and friends from Neurologisches Forschungshaus. We had a great time all together. Especially, I enjoyed the self-organized PhD meetings and the weekly Journal Club, as well as many other activities. I would also like to thank Hans Hintermaier and Andreas Häußler for their technical supports, and Katie Ogston for proofreading of manuscripts.

I thank all other friends in Munich, especially my previous colleges at TUM, and those from Chinese Scholarship Council funded students. They accompanied me through the years and made my life more diverse.

Last but not least, I want to express my deep love and heartfelt thankfulness to my family who care and support me unconditionally, as well as to my girlfriend Dr. Mingjing Zhu, who has been encouraging and supporting me all the time.

Publications

Peer-reviewed journals

Zhang L, Straube A, Eggert T (Submitted) Peripheral mechanisms compensate efficiently for small perturbations of arm movements. Motor Control

Zhang L, Straube A, Eggert T (2014) Torque response to external perturbation during unconstrained goal-directed arm movements. Experimental Brain Research 232 (4):1173-1184

Zhou T, **Zhang L**, Latash M (In press) Characteristics of unintentional movements by a multi-joint effector. Journal of Motor Behavior

Zhou T, **Zhang L**, Latash M (Submitted) Intentional and unintentional multi-joint movements: their nature and structure of variance. Neuroscience

Conference abstracts

Zhang L, Straube A, Eggert T (2014) Modulation of torque response to perturbations by changing feedback gains during arm reaching movements. Neural Control of Movement, Amsterdam, Netherlands

Zhang L, Eggert T, Straube A, Büttner U (2013) Short-latency torque response to external perturbation during complex arm reaching movements. Society for Neuroscience, San Diego, CA, USA

Zhang L, Eggert T, Glasauer S, Straube A (2012) Stiffness estimation during complex arm movements. Society for Neuroscience, New Orleans, LA, USA

Before the doctoral study

Zhang L, Zhang T, Wu H, Borst A, Kühnlenz K (2012) Visual Flight Control of a Quadrotor Using Bioinspired Motion Detector. International Journal of Navigation and Observation, vol. 2012

Eidesstattliche Versicherung

ZHANG, LEI

Name, Vorname

Ich erkläre hiermit an Eides statt,

dass ich die vorliegende Dissertation mit dem Thema

Rapid Motor Responses to External Perturbations During Reaching Movements:

Experimental Results and Modelling

selbständig verfasst, mich außer der angegebenen keiner weiteren Hilfsmittel bedient und alle Erkenntnisse, die aus dem Schrifttum ganz oder annähernd übernommen sind, als solche kenntlich gemacht und nach ihrer Herkunft unter Bezeichnung der Fundstelle einzeln nachgewiesen habe.

Ich erkläre des Weiteren, dass die hier vorgelegte Dissertation nicht in gleicher oder in ähnlicher Form bei einer anderen Stelle zur Erlangung eines akademischen Grades eingereicht wurde.

München, den 30.07.2015 Lei Zhang